Environmental Science and Ecotechnology 23 (2025) 100495

Contents lists available at ScienceDirect

Environmental Science and Ecotechnology

journal homepage: www.journals.elsevier.com/environmental-science-and-ecotechnology/

Review

Piezocatalysis for water treatment: Mechanisms, recent advances, and future prospects

Tian Jiang [a], Yuehan Wang [a], Chang Cai [a], Chunyang Nie [b, *], Honggen Peng [a], Zhimin Ao [c, **]

[a] School of Resources & Environmental, Nanchang University, Nanchang, 330031, China
[b] Research Institute of Interdisciplinary Sciences (RISE) and School of Materials Science & Engineering, Dongguan University of Technology, Dongguan, 523808, China
[c] Advanced Interdisciplinary Institute of Environment and Ecology, Beijing Normal University, Zhuhai, 519087, China

ARTICLE INFO

Article history:
Received 25 May 2024
Received in revised form
1 October 2024
Accepted 5 October 2024

Keywords:
Piezopotential
Mechanochemistry
Persulfate
Ultrasound

ABSTRACT

Piezocatalysis, which converts mechanical energy into chemical energy via the piezoelectric properties of materials, has emerged as a promising, eco-friendly technology for advanced oxidation processes in water treatment. It can be synergistically combined with other advanced oxidation techniques, such as photocatalysis and Fenton reactions, to enhance contaminant removal efficiency. In this Review article, we outline the fundamental principles of piezocatalysis, the mechanical energy sources employed, and recent advancements in piezocatalysis-coupled techniques for water decontamination. We systematically examine three potential mechanisms of piezocatalysis, assess the benefits and drawbacks of various mechanical energy inputs, and highlight the synergistic effects observed in combined systems. Furthermore, the review provides a roadmap for future research, emphasizing key areas such as piezocatalysis mechanisms, catalyst design, reactor architecture, and practical applications for water treatment. By offering a comprehensive analysis of current progress and challenges, this review is expected to stimulate further research into the theoretical and practical aspects of piezocatalysis-coupled technologies.

1. Introduction

Water is indispensable to life. However, modern society's rapid industrialization, urbanization, and population growth have led to an alarming accumulation of diverse inorganic and organic pollutants in the natural environment; this has resulted in a water crisis [1–3]. Therefore, effective technologies for water pollution control and improving wastewater reuse efficiency must be urgently developed.

Advanced oxidation processes (AOPs), which are based on reactive oxygen species (ROS), such as hydroxyl radical (•OH) and sulfate radical ($SO_4^{\bullet-}$), with higher oxidative capacity than a parent chemical oxidant, have been popularly adopted for the abatement of organic pollutants because they can quickly convert toxic organics into small organic molecules that are less toxic or nontoxic [4–6]. To evolve a considerable amount of reactive species for attacking organics, physical and chemical approaches, including light, electricity, and chemical catalysts, are exploited in AOPs to activate oxidants (e.g., O_2, O_3, hydrogen peroxide, Cl_2, persulfates) or even water [7–10].

Accordingly, diverse AOP technologies, such as photocatalytic oxidation, electrocatalytic oxidation, Fenton and Fenton-like reactions, and catalytic ozonation, have been applied for water remediation [11–16]. However, these technologies have limitations. For instance, the photocatalytic oxidation technique suffers from low solar energy conversion efficiency, the use of solar energy is affected by the weather, and ultraviolet (UV) light is generally utilized in practical applications, causing relatively high energy input. Fenton- and Fenton-like reactions usually require a large consumption of nonrenewable metal resources and have the risk of secondary pollution. These issues are not conducive to achieving

* Corresponding author.
** Corresponding author.
E-mail addresses: niechunyang@dgut.edu.cn (C. Nie), zhimin.ao@bnu.edu.cn (Z. Ao).

https://doi.org/10.1016/j.ese.2024.100495

the goal of carbon neutrality in the sewage treatment industry. In this context, developing new, green, energy-saving techniques to abate organic pollutants is in great demand.

In recent years, piezocatalysis has emerged as a hot topic in the field of catalysis because of its ability to harness environmental mechanical energy (e.g., water currents, tides, wind energy, noise) to drive a wide range of chemical reactions [17]. The principle of piezocatalysis is based on the piezoelectric effect, a physical phenomenon reported by the Curie brothers in France as early as 1880 [18]. They observed that when external stress was imposed on certain materials (piezoelectric materials), equal amounts of positive and negative charges appeared on their surfaces, with the surface charge density being proportional to the magnitude of the imposed force. Once the force was removed, the charges disappeared. Intrinsically, the appearance of polarized charges at the surface of deformed piezoelectric material results from the generation of a built-in electric field (piezopotential) inside a material, which is induced by a mismatch between the cation and anion centers within the unit cell of a piezoelectric crystal [19].

The piezoelectric effect has long been exploited in electromechanical sensors, actuators, self-powered nanogenerators, etc. [20,21]. Based on the peculiar properties of piezopotential, it is also utilized to manipulate the charge carrier transportation process in the surface/subsurface area and bulk phase of piezoelectric crystals, thus promoting catalytic activity [19]. In 2010, Xu's group at the University of Wisconsin reported for the first time that piezoelectric materials (ZnO microfibers and $BaTiO_3$ dendrites) dispersed in aqueous solution could catalyze the decomposition reaction of H_2O under ultrasonic sound, producing hydrogen and oxygen [22]. This pioneering work offered an avenue for the cost-effective production of clean energy to relieve environmental concerns about fossil fuels, thereby triggering scientific interest in piezocatalysis.

Over the past decades, the applications of piezocatalysis have flourished in the water-splitting area and many other areas, including environmental remediation, water disinfection, organic synthesis, bioapplications, and oxygen/CO_2 reduction reaction [23,24]. To date, a variety of piezocatalysts have been reported to show good degradation performances of aqueous organic contaminants, such as dyes, phenolic compounds, antibiotics, etc., via the production of ROS, such as •OH and superoxide radical ($O_2^{\bullet-}$) from piezo-driven hydrolysis reactions [25,26]. Moreover, the coupling of piezocatalysis with other advanced oxidation technologies, such as photocatalysis and Fenton-like reactions, attains an enhanced removal performance of organic pollutants by taking advantage of the piezopotential's ability to regulate the band structure and interfacial charge transfer process [27–30]. Hence, piezocatalysis can serve as a green, energy-saving, advanced oxidation technology and manifest great promise in practical water treatment.

Owing to recent progress in piezocatalysis, several reviews have introduced intrinsic piezocatalytic mechanisms and summarized the applications of piezocatalysis in the fields of water splitting, water remediation, and CO_2 reduction reactions in the literature. Some of these reviews focus on the performance of certain piezocatalysts [31–34] or individual piezocatalysis processes [35–41], and the rest concentrate on the coupled piezocatalytic techniques in which piezopotential is exploited to enhance the efficiency of other catalytic systems [42–48]. As for the latter, the published reviews primarily emphasize piezo-photocatalytic techniques due to the semiconducting feature of piezoelectric materials [44,45,47]. However, a growing number of articles reporting coupled piezocatalysis techniques with Fenton and Fenton-like reactions have been witnessed in recent years, while relevant reviews are rather limited. Therefore, this review presents recent advances in applying piezocatalysis and coupled piezocatalysis techniques in water remediation.

First, we introduce three possible proposed mechanisms of piezocatalysis, including energy band theory, electrocatalysis-like theory, and the screening charge effect. Then, we discuss the ways of initiating piezocatalysis. Following that, we summarize the research progress on the applications of piezocatalysis, coupled piezo-photocatalysis, piezo-Fenton, piezo-Fenton-like, and piezocatalysis coupled with persulfate-based AOPs (PS-AOPs) techniques in removing aqueous organic pollutants. Finally, we summarize and discuss the advantages and challenges of water treatment technology based on piezocatalysis.

2. The mechanism of piezocatalysis

Due to the asymmetric crystal structure of a piezocatalyst, the exertion of mechanical stress causes the positive and negative charge centers in the material to move about one another and produce net electric dipole moments. The superposition of these electric dipole moments leads to the formation of a piezopotential along the direction of the stress in a piezocatalyst, which lays the foundation of piezocatalysis because the piezopotential can alter the bandgap structure and surface charge distribution of a piezocatalyst. Currently, three plausible theories have been suggested to account for the mechanism of piezocatalysis: energy band theory, electrocatalysis-like theory, and the screening charge effect. For the three theories, the role that piezopotential plays in piezocatalytic reactions is different.

2.1. Energy band theory

Due to a certain degree of similarity between piezocatalysis and photocatalysis and the mature theories of photocatalysis and piezotronics, energy band theory can be adopted to partially explain the working principle of piezocatalytic reactions. In this theory, energized charge carriers from the piezocatalyst participate in the redox reaction, and the electronic state and bandgap structure are important factors regulating catalytic activities. However, differing from photocatalysis, the source of energized charge carriers and how charge carriers transfer and work in piezocatalysis are still debatable.

Two possible sources of charge carriers are proposed for piezocatalysis, including excited electron (e^-)/hole (h^+) pairs induced by mechanical energy excitation and the inherent free charge of a piezocatalyst (Fig. 1a and b). The production of free e^-/h^+ pairs from mechanical energy excitation in piezocatalysis resembles that

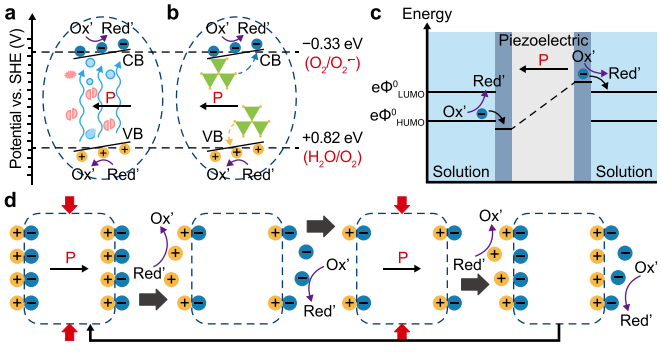

Fig. 1. **a**–**b**, Schematic diagrams of free carriers induced by mechanical excitation (**a**) and free carriers produced from the defects (**b**) in the piezocatalyst. VB: valence band, CB: conduction band. **c,** Schematic illustration of the principle of electrocatalysis-like theory. LUMO: lowest occupied molecular orbital, HUMO: highest occupied molecular orbital. **d,** Dynamic shielding phenomenon due to piezoelectric effect. P: the polarization field, Ox': oxidizing agent, Red': reducing agent.

in photocatalysis, i.e., mechanical energy can encourage the excitation of electrons from the valence band (VB) of a piezocatalyst to the conduction band (CB), leaving holes in the VB [49]. The occurrence of mechanical energy excitation is normally induced by ultrasonic waves as mechanical stress because the collapse of cavitation bubbles caused by ultrasonication can exert a pressure of up to 10^8 Pa on the heterogeneous catalyst/water interface, which provides sufficient energy for electron excitation.

Also, the ultrasonic cavitation bubbles would create a localized high temperature (~5000 °C), which might result in the thermal excitation of electrons [50]. Nevertheless, direct experimental evidence on producing free charges in a piezocatalyst under ultrasonic vibration is unavailable.

The inherent unpaired/free charges produced by flaws in the piezocatalyst can also serve as a source of free carriers. Especially when other types of mechanical energy with much lower intensity than ultrasound are applied to drive piezocatalytic reactions, the abovementioned mechanical energy excitation is unlikely to occur, and the inherent unpaired/free charges in the piezocatalyst are the main source of free carriers. As is known, the unpaired electrons or functional groups at the material's defects are intrinsically catalytic sites and can take part in specific chemical reactions [51]. For piezocatalysis, the piezopotential formed in the piezocatalyst can promote the migration of unpaired/free charges to the piezocatalyst surface and increase the surface concentration of free-charge carriers, thus facilitating the catalytic reaction [52]. On this basis, defect engineering has also been demonstrated to be an efficient approach to improving the activity of a piezocatalyst [53]. Anionic lattice defects, such as oxygen, selenium, and sulfur vacancies, are commonly present in piezocatalysts based on transition metal oxides and dihalides [54].

In photocatalysis, the match between the redox potentials of CB/VB and desired redox reactions (e.g., H_2O/O_2, $O_2/O_2^{\bullet-}$) is another prerequisite for initiating a photocatalytic reaction, which equally applies to piezocatalysis. In a deformed piezocatalyst, the generated piezopotential will bend the energy band (Fig. 1a and b) and change the redox potentials of free e^-/h^+ pairs, thus making them sufficiently negative or positive to trigger redox reactions [55,56]. It should be noted that the applied mechanical strain on the piezocatalyst must be periodic because the generated piezopotential would be gradually neutralized by the internal charges if the piezocatalyst is in a stable deformation state [57].

2.2. Electrocatalysis-like theory

The working principle of electrolysis can be briefly summarized as follows. The applied external electric potential onto the electrode can change the electronic energy levels of unoccupied states within the electrode, resulting in the transfer of electrons in the solution/electrode and triggering redox reactions [58]. For piezocatalysis, an induced piezopotential acts as the electric power source since its magnitude can reach as high as ten to hundreds of volts when moderate to severe stress is imposed [59]. Meanwhile, it is suggested that a generated piezopotential can change the bandgap of the piezocatalyst, contrasting with the case of the energy band theory that piezopotential tilts only the CB/VB energies of a piezocatalyst, and its bandgap remains unchanged (Fig. 1c). Accordingly, chemical species are adsorbed onto the surface of a piezocatalyst and then undergo redox reactions. In this scenario, the intrinsic free charges of piezocatalysts are deemed to act as the source of charge carriers in piezocatalysis.

Differing from electrocatalysis, the piezopotential will drop as the reactions proceed due to the capacitive and Faradaic effects, and the drop rate is suggested to depend on both the properties of piezoelectrics and the nature of a material's surrounding solution [60]. As mentioned earlier, piezopotential is periodically formed, thus guaranteeing the continuous occurrence of piezocatalytic reactions. Meanwhile, the equation describing mass transfer to the electrode in electrolysis still applies to piezocatalysis. On this basis, the expression of piezopotential as a function of time can be theoretically derived.

For instance, the expression proposed by Starr et al. well matched the measured voltage drop of piezopotential in a piezoelectric lead zirconate titanate ($Pb(Zr_xTi_{1-x})O_3$, PZT) material [59]. Moreover, the authors suggested that the piezocatalytic activity of different piezoelectric materials in terms of H_2 production is mainly determined by the piezoelectric moduli and relative permittivity of piezoelectrics, and related rate constants, which is consistent with the reported experimental results. Nevertheless, Starr et al. stated that the intrinsic free charges of the piezocatalyst can serve as effective screening agents of the piezopotential, and a free-charge concentration higher than the threshold value would induce a dramatic decrease in H_2 production efficiency [59]. This is contradictory to the generally acknowledged fact that increasing the concentration of free charges in the piezocatalyst via defect engineering is beneficial to catalytic efficiency. Additionally, whether the electrochemical frameworks are also applicable to other piezocatalytic reactions is unknown.

2.3. The screening charge effect

Like the electrolysis-like theory, the mechanism of the screening charge effect also highlights the dominating significance of piezopotential (i.e., piezopotential serves as the power source to attract external charges onto the surface of the deformed piezocatalyst). Nevertheless, those adsorbed external charges, which are known as screening charges, are deemed to be the free charges participating in redox reactions for the mechanism of the screening charge effect. The redox capacity of the adsorbed screening charge is comparable to that of the CB/VB edge in the piezocatalyst.

A piezocatalytic reaction based on the screening charge effect mechanism (Fig. 1d) can be briefly summarized as follows. (i) First, the surface of a piezocatalyst adsorbs screening charges from the surrounding medium when external stress is imposed. (ii) Then, the adsorbed screening charges are released from the surface of a piezocatalyst due to the vanishing of the internal electric field upon removing external stress. (iii) Oxidation-reduction reactions occur between the screening charges and certain substances in the surrounding medium (e.g., O_2, H_2O, persulfate molecule) because the redox capacity of the adsorbed screening charges is comparable to that of CB/VB edge in the piezocatalyst. (iv) When the external stress is applied again, the polarization of the piezocatalyst is reestablished, and screening charges in the surrounding medium are adsorbed on the surface of the piezocatalyst again, giving rise to the occurrence of redox reactions.

In other words, piezocatalytic reactions can be accomplished over piezoelectric materials through the continuous cycle of adsorption and desorption of surface screening charges induced by polarization [61]. Piezocatalytic efficiency is governed by the number of screening charges, which is closely related to the magnitude of piezopotential. However, whether the induced piezopotential would change the bandgap or bend the energy band in the mechanism of the screening charge effect remains unclear.

The three aforementioned mechanisms are still the subject of numerous debates, and they cannot satisfactorily explain some experimental phenomena. Further studies should be performed to fully understand the working principles of piezocatalysis and to offer a theoretical guide for advancing the use of piezocatalysis technology.

3. Types of mechanical energy utilized for piezocatalysis

Deformation of a piezoelectric material is first required to initiate the piezocatalytic reaction. According to the mechanism of piezocatalysis, the mechanical strain applied to the piezocatalyst should be periodic. Different types of mechanical energy, such as ultrasound waves, water flow, atmospheric pressure, and wind, can induce periodic deformation of a piezoelectric material. The commonly utilized ways to trigger piezocatalytic reactions for water decontamination include ultrasonic vibration, air bubbling, water-vortex disturbance, and ball milling (Fig. 2).

Ultrasound (US) is a high-frequency acoustic wave with good directionality, robust penetration, and a long transmission distance in water. The action of ultrasonography can cause the continuous formation of tiny cavitation bubbles in the liquid, and the collapsing of cavitation bubbles creates high pressure on the piezoelectric material to induce periodic deformation [62].

In a US-driven piezocatalytic system, several variables can affect catalytic efficiency, including US power, US frequency, and temperature. Normally, an increase in US power can enhance piezocatalytic efficiency. The US frequency has a significant impact on the vibration amplitude of a piezoelectric material, which is proportional to the strength of the piezoelectric effect. Previous studies discovered that the piezocatalytic efficiency reached its maximum when the US frequency met the resonance frequency of the piezocatalyst because the vibration amplitude was maximal at the resonance frequency [23]. Additionally, the solution temperature will rise continually during the US process, while temperature strongly influences many chemical reactions. Hence, proper regulation of temperature should be considered during the experimental process [63].

Although US can effectively trigger piezocatalytic processes and boost catalytic efficiency, it is rarely found in nature. The artificial creation of the US is energy intensive and can result in significant noise pollution. Furthermore, US waves are difficult to create in large channels and gradually decay in a turbid medium, limiting the widespread application of US-driven piezocatalysis [64].

The water bubble rupture driven by air bubbling or aeration is alternatively a low-frequency force [65–68]. Compared to US vibration, air bubbling offers softer stimuli but has lower energy consumption and less noise pollution. When the bubbles burst, the disappearance of the gas–liquid interface causes drastic changes and chemical energy release. In particular, aeration and air flotation processes are popular wastewater treatment methods [69], which make bubbling-driven piezocatalysis easy to fulfill in practical applications.

Additionally, the concentration of dissolved oxygen (DO) in water can be improved by air bubbling, and DO might be activated into ROS during the piezocatalysis process, thus promoting the removal efficiency of organic pollutants [67]. For instance, Hou et al. used air bubbling to drive the piezocatalytic degradation of antibiotics over coupling of expanded molybdenum disulfide and polyvinylidene fluoride (E-MoS_2/PVDF) microcapsules piezocatalyst [70]. The degradation efficiency of antibiotics over 85% was attained in 60 min. Importantly, the energy consumption of such an air-bubbling-driven piezocatalysis process (76.00 kWh^{-3} $order^{-1}$) was only 6.43% of US-driven piezocatalysis processes. Therefore, the air bubbling method provides a direction for reducing energy consumption and improving efficiency in water treatment.

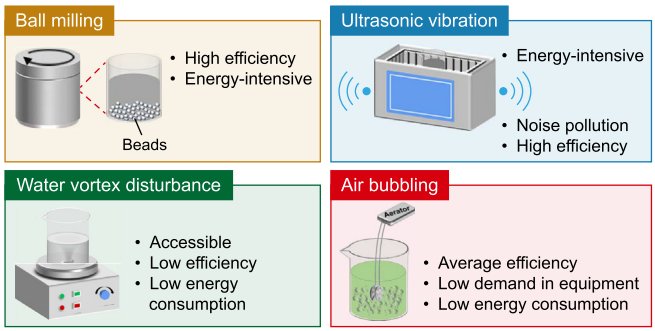

Fig. 2. Schematic diagrams of types of mechanical energy utilized for piezocatalysis.

Water-vortex disturbance is also a low-frequency mechanical force that commonly exists in nature. Hence, it can serve as a sustainable and green mechanical energy source for inducing the deformation of a piezocatalyst. It has been reported that piezoelectric materials, such as barium titanate and molybdenum disulfide, can harvest water vortex-induced by magnetic stirring and water flow in piping systems to trigger the piezocatalytic degradation of organic pollutants [66,71]. Based on the piezoelectric equation and Newton's rule of viscosity [72], the flow rate is an important factor affecting the efficiency of a water vortex-driven piezocatalytic system because the flow rate is positively correlated with the piezopotential. Therefore, with the rational design of a high-performance piezocatalyst and optimization of piping systems, the integration of piezocatalysis into current wastewater treatment processes to reduce the energy consumption of wastewater treatment plants is very appealing. However, even at very high speeds, the pressure of a water vortex acting on the surface of a piezocatalyst is significantly lower than that of ultrasound, resulting in lower catalytic efficiency.

The use of ball milling as mechanical energy for mechanochemical synthesis, such as the transformation of organic compounds and the creation of nanomaterials, has frequently been reported in the literature [73,74]. Ball milling produces frictional heat that can quickly raise the local temperature to hundreds or thousands of degrees Celsius. This high energy can cause various reactions, including breaking or forming chemical bonds, crushing particles into minuscule sizes, and forming crystallographic defects in the particles [75]. As a result, ball milling has also been employed as a mechanical force in piezocatalysis. For instance, Meng et al. prepared a Fe@3D-WS_2 nanoflowers (NFs) piezocatalyst to degrade levofloxacin (LEVO) by wet ball milling [76]. Their findings revealed that LEVO was efficiently degraded over Fe@3D-WS_2 NFs under the ball milling agitation. Moreover, ball milling is advantageous to US vibration in promoting the stability of Fe@3D-WS_2 NFs, ascribed to the reason that catalytic sites in the piezocatalyst were self-renewed by ball milling.

In summary, compared to air bubbling and water vortexing, US and ball milling are more efficient ways to trigger piezocatalytic reactions due to the higher mechanical energy supply, while they are more energy intensive and unsuitable for large-scale water treatment. Air bubbling and water vortex as ubiquitous mechanical energy show great potential in driving piezocatalysis for practical water remediation. Improving the catalytic efficiency of low-frequency force-driven piezocatalysis remains a big challenge. However, an involved catalytic mechanism and an organic pollutant degradation mechanism might differ when the utilized mechanical energy is distinct. For instance, in the US-driven piezocatalytic system, sonolysis may partially contribute to the degradation of organic pollutants, and the resulting degradation pathway may differ from that of the water vortex-driven piezocatalytic system.

In the air-bubbling-driven piezocatalytic system, the high concentration of DO can be activated into $O_2^{\bullet-}$ via piezocatalysis, while the organic pollutant degradation pathway caused by $O_2^{\bullet-}$ perhaps differs from that caused by •OH. Additionally, the organic pollutant

oxidation processes in the air-bubbling-driven piezocatalytic system mainly occur at a three-phase (gas, solid, and liquid) interface, whose properties are distinct from those of the solid-liquid interface present in water vortex/ball milling-driven piezocatalytic systems. Such differences can significantly affect the thermodynamics of organic pollutant oxidation reactions.

4. Applications of piezocatalysis and coupled piezocatalysis techniques in water decontamination

Owing to the redox capability of free-charge carriers/screening charges and the peculiar ability of piezopotential in regulating the band structure and charge transportation, the deformed piezocatalyst can react with H_2O/O_2 molecules to evolve highly reactive species [41]. Therefore, piezocatalysis has emerged as an efficient AOP for the abatement of organic pollutants. Meanwhile, the pollutant removal performance of piezocatalysis can be enhanced by coupling with other AOP techniques due to the functions of piezopotential and piezo-induced free-charge carriers/screening charges in various chemical reactions.

In particular, the synergistic effect of piezocatalysis-coupled AOP techniques significantly promotes the catalytic efficiency and degradation of organic pollutants. To date, it has been demonstrated that piezocatalysis can be coupled with photocatalysis, Fenton and Fenton-like oxidation, and PS-AOPs to achieve enhanced removal of organic pollutants. In this section, the organic pollutant removal mechanisms involved in piezocatalysis, piezo-photocatalysis, piezo-Fenton, piezo-Fenton-like, and piezo-PS-AOP technologies are discussed, and their applications in water remediation are summarized.

4.1. Piezocatalysis technology

Although the intrinsic mechanism of piezocatalysis is not fully understood by far, the primary reactions occurring in the piezocatalytic oxidation of organic pollutant processes can be briefly described by equations (1)–(5) and Fig. 3a: (i) the piezocatalyst is polarized by external mechanical energy to generate piezopotential and piezo-induced e^- and h^+; (ii) piezo-induced e^- then reacts with dissolved O_2 to produce $O_2^{\bullet-}$ and piezo-induced h^+ interacts with H_2O to produce •OH; (iii) the interaction between $O_2^{\bullet-}$ and •OH may generate $^1O_2$ and the interaction between $O_2^{\bullet-}$ and H^+ may generate H_2O_2; (iv) finally the evolved ROS and piezo-induced h^+ oxidize the organic pollutant.

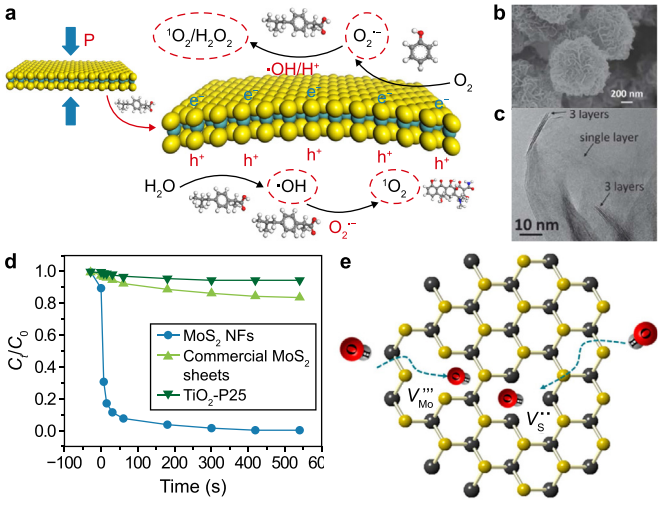

Fig. 3. **a**, Schematic diagram of piezocatalytic degradation of organic pollutants. P: the polarization field. **b**–**c,** Scanning electron microscopy (**b**) and transmission electron microscopy (**c**) images of single and few-layered MoS_2 nanoflowers (NF). **d,** Degradation performance of rhodamine B using the MoS_2 nanoflowers piezocatalyst under ultrasound vibration in the dark. Adapted with permission from Ref. [84], Copyright 2016, Wiley. **e,** Illustration of the accommodation of •OH on the F-centers defects in MoS_2 nanoflowers such as M-(V_{Mo}''') and S-vacancies ($V_S^{\bullet\bullet}$). Reprint with permission from Ref. [89], Copyright 2018, Elsevier.

$$\text{Piezocatalysis} + \text{Mechanical energy} \rightarrow e^- + h^+ \quad (1)$$

$$e^- + O_2 \rightarrow O_2^{\bullet-} \quad (2)$$

$$h^+ + H_2O \rightarrow \bullet OH + H^+ \quad (3)$$

$$O_2^{\bullet-} + \bullet OH \rightarrow OH^- + {}^1O_2 \quad (4)$$

$$O_2^{\bullet-} + 2H^+ \rightarrow H_2O_2 \quad (5)$$

In the earlier research on piezocatalytic oxidation of organic contaminants in water, traditional piezoelectric materials, such as PZT, $BaTiO_3$, and ZnO, were widely utilized as catalysts. The organic pollutants were targeted at dyes like rhodamine B (RhB), acid orange (AO7), methyl orange (MO), methylene blue (MB), and methyl violet (MV) (Table 1) [77]. For instance, Hong et al. demonstrated that an AO7 removal efficiency of ~90% was attained within 80 min by $BaTiO_3$ microdendrites under US vibration [63], and the primary cause of AO7 degradation is •OH. As more research has progressed, novel piezoelectric materials, such as two-dimensional transition metal dichalcogenides (TMDCs) and bismuth-based compounds, have been employed to degrade various types of organic pollutants besides dyes (e.g., phenols, antibiotics, carbamazepine (CBZ), etc.) [78].

For example, Wu et al. prepared single- and few-layered MoS_2 NFs and investigated their piezocatalytic performance in degrading RhB under US vibration in the dark [84]. The as-prepared MoS_2 NFs piezocatalyst achieved a degradation efficiency of 93% within 60 s with a much higher specific rate constant than the reported values (Fig. 3b–d). The extraordinary piezocatalytic activity of MoS_2 NFs is attributed to the abundant presence of single layers and odd-numbered layers that are piezoelectric. More importantly, Wu et al. discovered that F-center defects at the edges of MoS_2 nanosheets, which were formed by MO and S vacancies (Fig. 3e), could bond with •OH evolved from the piezocatalytic water-splitting reactions, which significantly prolongs the lifetime of •OH and thus enhances the degradation of RhB [89].

Since piezoelectric materials are intrinsically semiconducting, their charge carrier mobility is lower than that of metallic materials, which limits piezocatalytic activity. To overcome this problem, researchers have made various modifications to piezoelectric materials involving defects engineering, phase engineering, doping, and compounding with other materials [86]. For instance, Pan et al. fabricated a barium titanate and graphene composite ($BaTiO_3$@G) material and utilized it as the piezocatalyst for the decomplexation of Cu-ethylenediamine (Cu-EDTA) [90]. Compared to pristine $BaTiO_3$, the $BaTiO_3$@G exhibited a much higher Cu-EDTA degradation efficiency under US vibration (Fig. 4a), demonstrating that compounding $BaTiO_3$ with metallic graphene is an efficient way to improve its piezocatalytic activity. Meanwhile, the free Cu(II) ions resulting from the decomplexation of Cu-EDTA were readily adsorbed by the residual oxygenated groups on graphene, enabling simultaneous piezocatalytic decomplexation and resource recovery *in situ*. Furthermore, Pan et al. shaped the powdery $BaTiO_3$@G into a three three-dimensional millimeter-sphere and filled the beads into a glass column reactor to assess the application potential of piezocatalysis in the treatment of heavy metal complexes (Fig. 4b).

Table 1
Applications of piezoelectric materials in piezocatalytic degradation of organic pollutants.

Materials	Contaminant	k_{obs} (min^{-1})	ROS	Conditions	Reference
$BaTiO_3$ nanosheets	RhB	0.13	•OH and $O_2^{\bullet-}$ accounted for RhB oxidation	US (100 W, 40 kHz)	[79]
$BaTiO_3$ dendrites	AO7	0.05	•OH accounted for AO7 oxidation	US (80 kHz)	[63]
$BaTiO_3$ nanoparticles	MO	0.02	•OH, $O_2^{\bullet-}$, and h^+ accounted for MO oxidation	US (80 W, 40 kHz)	[62]
ZnO nanoparticles	MB	0.01	•OH and $O_2^{\bullet-}$ accounted for MB oxidation	US (150 W, 40 kHz)	[80]
ZnO nanorods	AO7	0.03	•OH accounted for AO7 oxidation	Vibration	[81]
$BiFeO_3$ nanowires	RhB	0.04	•OH and h^+ accounted for RhB oxidation	US (80 W, 132 kHz)	[82]
$BiFeO_3$ nanosheets	RhB	0.01	•OH and h^+ accounted for RhB oxidation	US (80 W, 132 kHz)	[82]
$Bi_4Ti_3O_{12}$ nanoplates	RhB	0.06	•OH and $O_2^{\bullet-}$ accounted for RhB oxidation	US (80 W, 40 kHz)	[83]
MoS_2 nanoflowers	RhB	3.06	•OH, $O_2^{\bullet-}$, and H_2O_2 accounted for RhB oxidation	US (250 W, 40 kHz)	[84]
$MoSe_2$ nanoflowers	RhB	3.45	•OH, $O_2^{\bullet-}$, and H_2O_2 accounted for RhB oxidation	US (250 W, 40 kHz)	[85]
WS_2 nanoflowers	RhB	1.15	•OH, $O_2^{\bullet-}$, and H_2O_2 accounted for RhB oxidation	US (30 W, 40 kHz)	[86]
$NaNbO_3$ nanowires	RhB	0.01	•OH accounted for RhB oxidation	US (40 kHz)	[87]
$Pb(Zr_{0.52}Ti_{0.48})O_3$ nanowires	MO	0.02	•OH and $O_2^{\bullet-}$ accounted for MO oxidation	US (120 W, 40 kHz)	[88]
$Pb(Zr_{0.52}Ti_{0.48})O_3$	AO7	0.03	Not investigated	US (40 kHz)	[25]
$Cd_4BiO(BO_3)_3$	CBZ	0.06	•OH and e^- accounted for CBZ oxidation	US (120 W, 40 kHz)	[78]

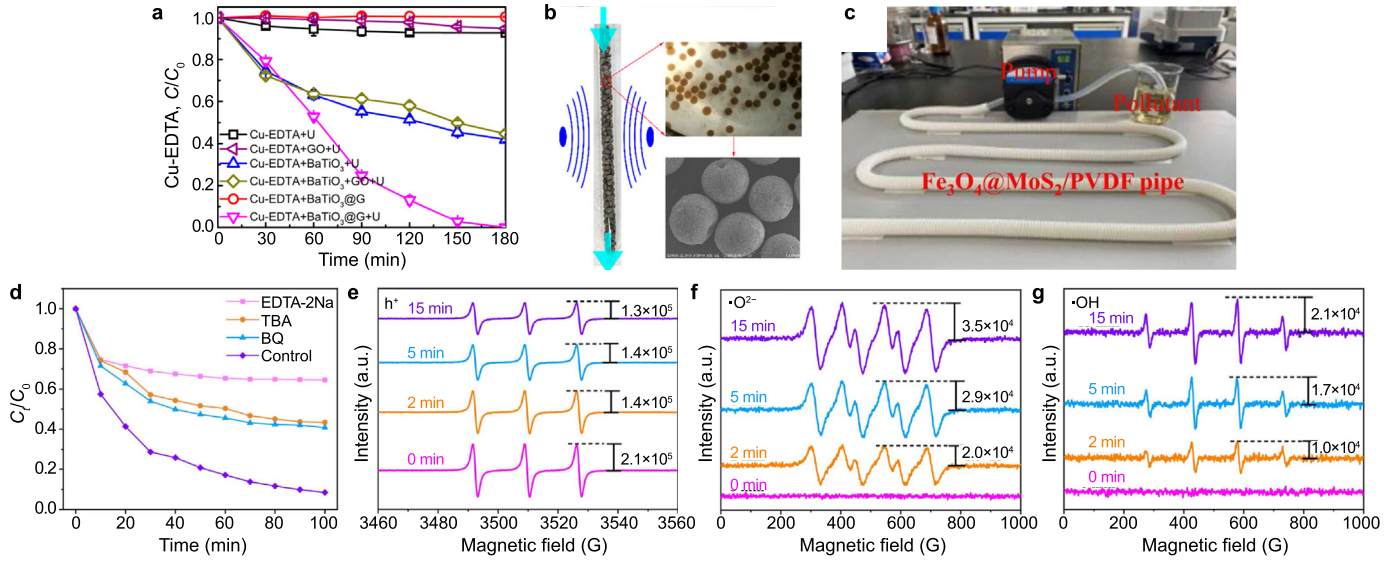

Fig. 4. a, Decomplexation efficiency of Cu-ethylenediamine (Cu-EDTA) under different conditions. GO: graphene oxide, U: Ultrasound. **b,** $BaTiO_3$ nanowires compounded with graphene ($BaTiO_3$@G) gel sphere column. Adapted with permission from Ref. [90], Copyright 2019, ACS Publications. **c,** Actual photo of an experimental device for the degradation of organics by Fe_3O_4@MoS_2/PVDF pipe. PVDF: polyvinylidene fluoride. **d**–**g**, Scavenging experiments (**d**), electron paramagnetic resonance spectra of h^+ (**e**), electron paramagnetic resonance spectra of $O_2^{\bullet-}$ (**f**), and electron paramagnetic resonance spectra of •OH (**g**) for the piezocatalytic degradation of tetracycline over Fe_3O_4@MoS_2/PVDF pipe. EDTA-2Na: ethylenediaminetetraacetic acid disodium salt. TBA: tert-butanol, BQ: benzoquinone. Adapted with permission from Ref. [91], Copyright 2023, Elsevier.

It was found that the degradation efficiency of Cu-EDTA by the piezocatalytic reactor was up to 78.1% under continuous flow mode. The adsorbed Cu ions could be easily recovered by HCl solution.

Recently, Wang et al. prepared a novel Fe_3O_4@MoS_2/PVDF modified pipe and used it for self-powered piezocatalytic degradation of organics in the pipeline via collecting energy from water flow (Fig. 4c) [91]. It was found that the modifications with Fe_3O_4 and MoS_2 remarkably increased the content of β phase of PVDF, thus elevating the piezoelectric response of Fe_3O_4@MoS_2/PVDF about pure PVDF. As a consequence, the Fe_3O_4@MoS_2/PVDF pipe manifested a higher tetracycline (TC) removal efficiency of 92.5% within 60 min than the pure PVDF, Fe_3O_4/PVDF, and MoS_2/PVDF pipes. The piezocatalytic pipe system was also able to effectively degrade other types of organic pollutants, including RhB, ciprofloxacin, and oxytetracycline, with efficiencies of 90.9%, 85.9%, and 69.2%, respectively. Moreover, the degradation performance of Fe_3O_4@MoS_2/PVDF marginally changed after six cyclic tests, indicating its good stability. The dominant ROS accounting for TC oxidation in the piezocatalytic Fe_3O_4@MoS_2/PVDF pipe system was revealed to be •OH, $O_2^{\bullet-}$, and piezo-induced h^+ based on the results of electron paramagnetic resonance spectroscopy (EPR) analysis and quenching tests (Fig. 4d–g). The outcomes of this work demonstrate the promising potential of harnessing hydromechanical energy for the piezocatalytic degradation of organic pollutants.

4.2. Piezo-photocatalysis technology

Photocatalysis, which can harvest solar energy to drive redox reactions, has been popularly applied in water remediation and many other areas, such as air pollution control, water splitting, organic synthesis, etc. [92–96]. However, the quick recombination of photogenerated electrons and holes when they diffuse onto the photocatalyst surface substantially reduces the photocatalysis effectiveness [97]. Thanks to the capacity of piezopotential to manipulate the charge carrier transportation process, the combination of piezocatalysis with photocatalysis is a promising route for enhancing the quantum efficiency of photocatalysis [98,99]. Most

piezoelectric materials also show photocatalytic activity, and they may directly exploit the built-in electric field to separate photo-induced charge carriers during the light/piezo-excitation (known as the piezophototronic effect), which is conducive to the abatement of organic pollutants [100]. Therefore, piezo-photocatalysis has been the subject of numerous investigations in recent years because it can simultaneously convert mechanical and solar energy into chemical energy (Table 2).

The primary reactions occurring in the piezo-photocatalytic oxidation of organic pollutant processes are illustrated in Fig. 5a. (i) Under light irradiation, the photocatalyst would absorb phonons and electrons in the VB are excited to the CB, producing photo-induced e^-/h^+ pairs. (ii) Meanwhile, a built-in electric field is formed in a piezocatalyst when an external stress is applied, which can separate the photoinduced e^-/h^+ pairs and reduce the recombination rate. (iii) Then photo-induced e^- reacts with dissolved O_2 to evolve $O_2^{\bullet-}$ and photo-induced h^+ interacts with H_2O to evolve •OH. (iv) Finally the generated ROS and photo-induced h^+ oxidize the organic pollutant. It should be noted that piezo-induced e^-/h^+ pairs also interact with O_2/H_2O during piezo-photocatalytic processes, but they only make a minor contribution to organic oxidation.

For instance, an Ag_2O-$BaTiO_3$ nanocomposite photocatalyst was prepared by Li and co-workers aiming to exploit the piezopotential formed in $BaTiO_3$ for separating photogenerated e^-/h^+ pairs and thus improve the photocatalytic activity of Ag_2O [102]. Under the combined light and ultrasonic irradiation, Ag_2O-$BaTiO_3$ achieved an RhB degradation efficiency of ~90% within 1 h, while the single photocatalytic (light irradiation alone) and piezocatalytic (US alone) systems only achieved degradation efficiencies of ~66% and ~10%, respectively (Fig. 5b). Additionally, the formation of a built-in electric field in Ag_2O-$BaTiO_3$ can also suppress the formation of elemental silver from the reactions between electrons and Ag^+ and thus improve the reusability of Ag_2O in terms of the sonophotocatalytic degradation of RhB.

Recently, Lv et al. prepared a novel bamboo-like $BaTiO_3$//ZnO Janus nanofibers PVDF membrane (BTO//ZO JNM) and utilized it for piezo-photocatalytic removal of multiple pollutants from water (Fig. 6a–e) [110]. Both the piezoresponse force microscopy (PFM) measurement and finite element simulation results revealed that BTO//ZO JNM possesses good piezoelectric properties and that a large piezopotential was caused under external pressure, which is conducive to piezo-photocatalysis. Accordingly, under concurrent light irradiation and magnetic stirring, photo/piezo-induced e^- in BTO//ZO JNM rapidly reacted with O_2 to form a considerable amount of $O_2^{\bullet-}$, resulting in efficient degradation of various organic contaminants, including TC, bisphenol A (BPA), congo red, and MB, even with the interference of low concentration of Ni^{2+} or Cu^{2+}. Meanwhile, only a small fall in the piezo-photocatalytic degradation efficiency was observed for BTO//ZO JNM after six cycles,

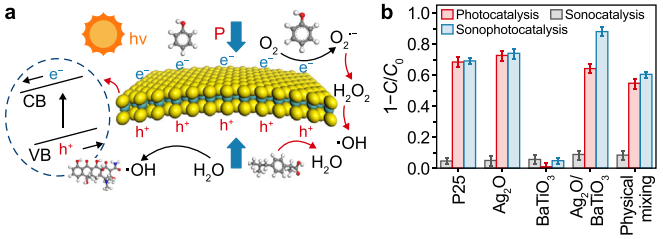

Fig. 5. a, Schematic illustration of the principle of piezo-photocatalysis. hv: illumination or ultraviolet irradiation, P: the polarization field, VB: valence band, CB: conduction band. **b,** Sonophotocatalytic, photocatalytic, and sonocatalytic degradation rate of rhodamine B over Ag_2O-$BaTiO_3$ photocatalyst and control samples. Adapted with permission from Ref. [102], Copyright 2015, ACS Publications.

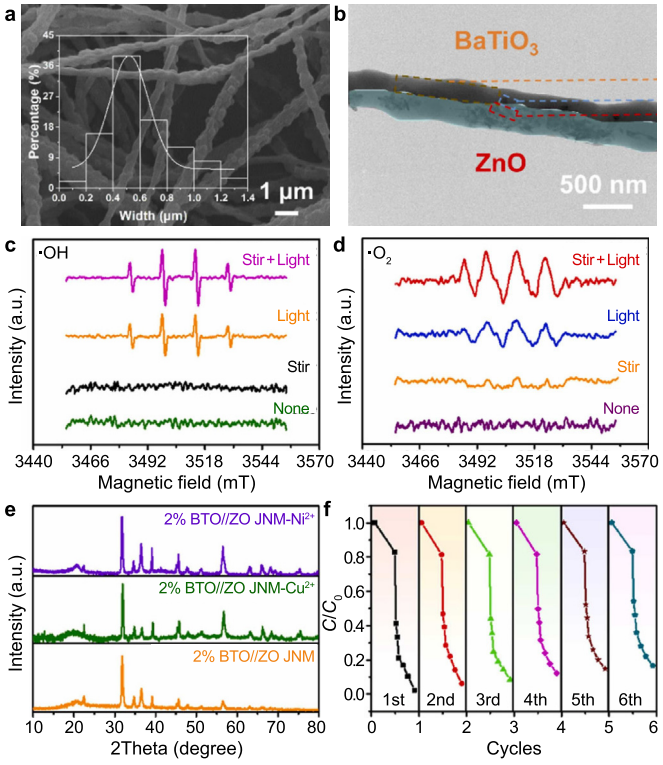

Fig. 6. a–b, Scanning electron microscopy (**a**) and transmission electron microscopy (**b**) images of $BaTiO_3$//ZnO Janus nanofibers PVDF membrane (BTO//ZO JNM). **c–d,** Electron paramagnetic resonance spectra of •OH (**c**) and $O_2^{\bullet-}$ (**d**) analysis on the generated reactive oxygen species in the piezo-photocatalytic system based on BTO//ZO JNM. **e,** X-Ray diffraction patterns of BTO//ZO JNM after six cycles of recovery. **f,** Cyclic tetracycline removal tests using BTO//ZO JNM in Ni^{2+} solution. Adapted with permission from Ref. [110], Copyright 2023, Elsevier.

Table 2
Applications of piezoelectric materials in piezo-photocatalytic degradation of organic pollutants.

Materials	Contaminant	k_{obs} (min^{-1})	Mechanism	Conditions	Reference
ZnO	RhB	0.03	Not investigated	UV (365 nm, 100 W) and stir (1000 rpm)	[101]
$Ag_2O/BaTiO_3$	RhB	Unavailable	Not investigated	Mercury lamp (365 nm) and US (50 W, 27 kHz)	[102]
BiOCl	RhB	0.03	h^+ and $O_2^{\bullet-}$ accounted for RhB oxidation	Xe lamp (>420 nm, 300 W) and US (~120 W, 40 kHz)	[103]
CuS/ZnO	MB	0.18	h^+, •OH, and $O_2^{\bullet-}$ accounted for MB oxidation	Xe lamp (200–1100 nm, 500 W) and US (200 W)	[104]
$KNbO_3$	RhB	0.02	•OH and $O_2^{\bullet-}$ accounted for RhB oxidation	Xe lamp (300 W) and US (110 W, 40 kHz)	[98]
Bi_2MoO_6/BiOBr	MV	0.03	h^+, •OH, and $O_2^{\bullet-}$ accounted for MV oxidation	Metal halide lamp (400 W) and US	[105]
BiOBr	RhB	0.07	h^+, •OH, and $O_2^{\bullet-}$ accounted for RhB oxidation	White light emitting diode (LED, 9 W) and US (120 W, 40 kHz)	[106]
Bi_2WO_6	RhB	0.14	•OH and $O_2^{\bullet-}$ accounted for RhB oxidation	White LED (9 W) and US (120 W, 40 kHz)	[107]
$Bi_{0.5}Na_{0.5}TiO_3$	RhB	0.06	•OH and $O_2^{\bullet-}$ accounted for RhB oxidation	Xe lamp (300 W) and US (110 W, 40 kHz)	[108]
PAN/TiO_2	RhB	0.05	•OH and $O_2^{\bullet-}$ accounted for RhB oxidation	Xe lamp (350 W) and US (110 W, 40 kHz)	[109]
$BiFeO_3$	RhB	0.06	h^+, •OH, and $O_2^{\bullet-}$ accounted for RhB oxidation	Xe lamp (300 nm < λ < 600 nm, 300 W) and US (80 W, 132 kHz)	[82]

indicating good stability (Fig. 6f). Therefore, BTO//ZO JNM shows good promise in harvesting solar light energy and environmental vibrations for practical wastewater treatment.

4.3. Piezo-fenton and piezo-fenton-like oxidation technology

As the most classic AOPs, Fenton processes have been widely used in practical wastewater treatment due to the production of •OH from the reactions between Fe^{2+} ion and H_2O_2 [111]. H_2O_2 may also be generated during piezocatalytic water-splitting reactions, but it was not effectively utilized during the piezocatalytic degradation processes because H_2O_2 itself shows the limited oxidative ability of organic pollutants (Fig. 3) [112,113]. To improve the degradation performance of a piezocatalytic system, researchers proposed adding Fe^{2+} into the system to activate the *in situ* generated H_2O_2 to obtain more ROS (Fig. 7a) [114]. In particular, H_2O_2 is an unstable liquid oxidant with high transportation and storage costs, while the *in situ* synthesis of H_2O_2 offers a feasible way to overcome this drawback. For instance, several studies detected the *in situ* generation of H_2O_2 in a piezocatalytic $BaTiO_3$/US system, and the H_2O_2 yield was affected by US power and catalyst dosage [115]. Meanwhile, the addition of Fe^{2+} into the $BaTiO_3$/US system significantly improves the piezocatalytic degradation efficiency of several types of organic pollutants (e.g., dyes, phenol, 4-chlorophenol, etc.) due to the production of •OH from a Fenton reaction. Interestingly, it was found that the piezocatalytic degradation efficiency attained by $BaTiO_3$/US system increases with the molecular weight of the organic dye.

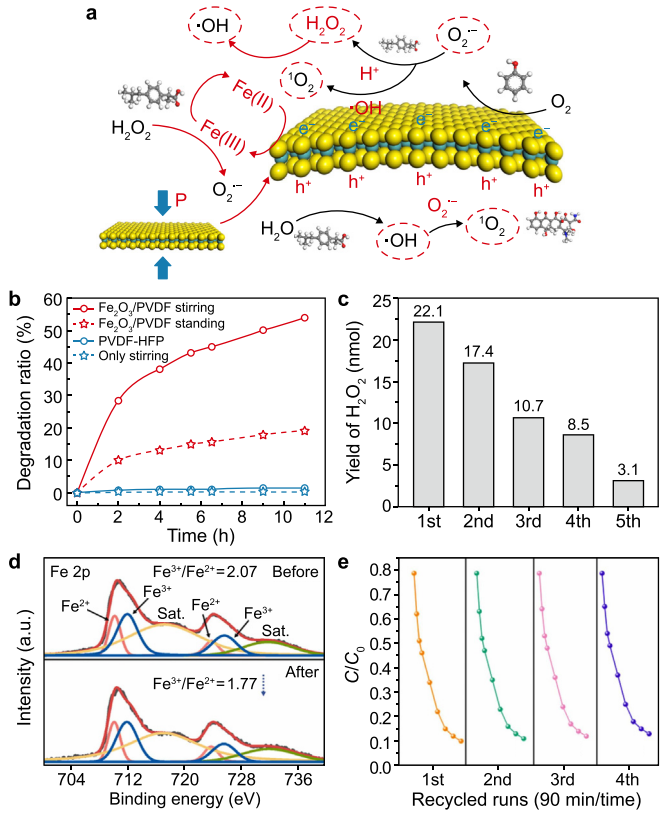

Fig. 7. a, Schematic illustration of the piezo-Fenton/Fenton-like oxidation principle. P: the polarization field. **b,** Tetracycline degradation ratio attained by Fe_2O_3-modified polyvinylidene fluoride-hexafluoro propylene (Fe_2O_3/PVDF-HFP) and PVDF-HFP porous films under different conditions. **c,** H_2O_2 yield in cyclic tetracycline removal tests with Fe_2O_3/PVDF-HFP. **d,** X-ray photoelectron spectroscopy spectra of fitted Fe 2p peak points for the Fe_2O_3/PVDF-HFP before and after the degradation experiment. Adapted with permission from Ref. [118], Copyright 2022, Elsevier. **e,** Cycling sildenafil removal tests using Fe_3O_4 piezocatalyst. Adapted with permission from Ref. [123], Copyright 2023, Elsevier.

Apart from aqueous Fe^{2+}, Fe-based compounds are also effective catalysts for H_2O_2 activation [116]. Compared to the homogeneous Fe^{2+} catalyst, heterogeneous Fe-based metallic catalysts have a wider adoptive pH range and are more conducive to recovery, therefore attracting huge attention [117]. Hence, many studies have also reported the application of Fe-modified piezoelectric materials in piezo-Fenton-like oxidation technology [118]. In particular, some Fe-containing piezoelectric materials also show chemical activity toward H_2O_2 activation, and they can serve as a multifunctional material in piezo-Fenton-like oxidation technology [119]. Another benefit brought about by the coupling of piezocatalysis with Fenton-like oxidation based on Fe-based piezocatalytic materials is that piezo-induced e^- can accelerate the redox Fe^{2+}/Fe^{3+} cycle involved in Fenton processes, which remarkably improves ROS production and catalyst stability (Fig. 7a) [120]. It should be noted that, in several studies, external H_2O_2 was also added to the piezo-Fenton-like system to enhance the elimination of organic pollutants, as the amount of *in situ* generated H_2O_2 is relatively limited [118].

Thus far, Fe-doped g-C_3N_4 [121], Fe-doped $BiVO_4$ [114], Fe_2O_3-modified PVDF-hexafluoro propylene (α-Fe_2O_3/PVDF-HFP) membrane [118], nanostructured $FeWO_4$, MoS_2/α-Fe_2O_3 heterojunction [122], Fe_3O_4 coated conductive carbon modified tourmaline (Tml@C@Fe_3O_4) [120] and mesoporous Fe_3O_4 with large surface undulations [123] have been utilized as piezocatalysts in piezo-Fenton-like systems. For example, the flexible Fe_2O_3/PVDF-HFP membrane manifests a TC degradation efficiency of 53.7% under flowing water with magnetic stirring, which is 37 times higher than that achieved by the PVDF-HFP membrane (1.4%) under stirring (Fig. 7b) [118].

The enhanced degradation performance of Fe_2O_3/PVDF-HFP membrane is attributed to several reasons: (i) the incorporation of α-Fe_2O_3 nanoparticles into the PVDF membrane increased the specific surface area and piezoelectric β-phase content of the PVDF membrane, resulting in promoted piezocatalytic activity of the membrane; (ii) Fe_2O_3 can effectively activate the *in situ* generated H_2O_2 (Fig. 7c) to evolve more ROS for attacking TC; (iii) the H_2O_2 activation efficiency over Fe_2O_3 was further boosted by the accelerated Fe^{3+} reduction over piezo-induced e^-, which was verified by an X-ray photoelectron spectroscopy (XPS) analysis and testing TC removal efficiency by Fe_2O_3/PVDF-HFP membrane with external H_2O_2 addition in a standing state (without stirring) (Fig. 7d). Among these factors, the improved piezocatalytic activity of Fe_2O_3/PVDF-HFP played a major role in TC removal because the authors found that the H_2O_2 yield decreased by 85% after five consecutive degradation cycles, but the TC degradation efficiency decreased only by 15% (Fig. 7c). Additionally, the results of the quenching tests and EPR analysis revealed that $O_2^{\bullet-}$ produced from the piezocatalytic oxidation of water and H_2O_2 activation over Fe_2O_3 is the main ROS responsible for TC degradation.

Fe_3O_4, as a non-piezoelectric material, has been popularly used as a catalyst for H_2O_2 activation, while it has the drawback of poor stability [124]. Interestingly, Jia et al. synthesized three-dimensional mesoporous Fe_3O_4 with defective oxygen atoms and large surface undulations and demonstrated that the as-prepared Fe_3O_4 material showed good sildenafil degradation performance and reusability in piezo-Fenton-like oxidation technology [123]. The PFM measurements confirmed that the as-prepared Fe_3O_4 shows a good piezoelectric response. Meanwhile, a degradation efficiency of 30% attained by Fe_3O_4 under US vibration also indicated that it has piezocatalytic activity, which is ascribed to the reason that the mesoporous pore channels and large surface

undulations of as-prepared Fe_3O_4 can enhance the US cavitation effect and thus the piezoelectric effect. With an external H_2O_2 addition, the Fe_3O_4-based piezo-Fenton-like system exhibited a higher degradation efficiency of ~91%, assigning to the efficient H_2O_2 activation over Fe_3O_4 to evolve more •OH as the primary ROS for sildenafil oxidation.

Moreover, the as-prepared Fe_3O_4 catalyst can be used repeatedly for contaminant removal under US vibration, and its degradation performance marginally declined after four cycles (Fig. 7e). By employing XPS techniques to examine the proportions of Fe^{2+} and Fe^{3+} in fresh and used Fe_3O_4 catalyst, it was found that the Fe^{3+} content was decreased and Fe^{2+} content was increased in the used Fe_3O_4 catalyst with regard to fresh sample. This supports the idea that piezo-induced e^- accelerates the transformation of Fe^{3+} into Fe^{2+} and thus improves the stability of Fe_3O_4. However, the origin of piezoelectricity in Fe_3O_4 prepared in this work was not fully understood, and further research is required to consolidate that constructing mesoporous materials with large surface undulations is a feasible approach to improving piezoelectricity in Fe_3O_4.

4.4. Piezocatalysis coupled with PS-AOP technology

Over the last two decades, the use of persulfate (including peroxymonosulfate (PMS) and peroxydisulfate (PDS)) as a superoxide precursor to produce sulfate radicals ($SO_4^{\bullet-}$) has been extensively investigated in AOPs [125]. Compared to •OH, $SO_4^{\bullet-}$ has a higher redox potential (1.8–2.7 V for •OH and 2.5–3.1 V for $SO_4^{\bullet-}$), a longer half-life time (30–40 μs for $SO_4^{\bullet-}$ and <1 μs for •OH) and a wider pH operating range, which facilitate the degradation of organic pollutants [126,127]. Also, persulfate is a solid oxidant that is less expensive to transport and store than H_2O_2. Therefore, researchers are considering the feasibility of PS-AOPs in actual wastewater treatment. Differing from H_2O_2, persulfate can be piezocatalytically activated to evolve ROS, probably due to the smaller peroxide O–O bond dissociation energy of persulfate [128]. Therefore, coupling piezocatalysis with PS-AOPs for water remediation has attracted much interest.

Studies on the piezocatalytic activation of persulfate have been relatively limited compared to persulfate activation by other methods, and the involved catalytic mechanism is not fully understood, while researchers prefer to adopt energy band theory to explain the observed relevant phenomena. Upon the exertion of mechanical stress, piezo-induced e^- in a deformed piezocatalyst reacts with PMS/PDS molecule to produce free radicals ($SO_4^{\bullet-}$ and •OH), and piezo-induced h^+ reacts with PMS/PDS molecule to produce $SO_5^{\bullet-}$ and H^+ (Fig. 8a). Then, the combination of two $SO_5^{\bullet-}$ leads to the formation of a $SO_4^{\bullet-}$, $SO_4^{\bullet-}$ can react with H_2O molecules to produce •OH. At the same time, the piezocatalytic water-splitting reactions (Fig. 8a) also occur in a piezo-activated PS-AOP system. For the piezocatalyst, which also has chemical activity toward PS activation, its intrinsic free charges react with the PS molecule to generate reactive species during the piezocatalytic activation process. In particular, piezo-induced e^- can regenerate metallic active sites ($M^{n+}/M^{(n+1)+}$) in the piezocatalyst, thus enhancing PS activation efficiency and catalyst stability [129]. Finally, the as-produced reactive species and piezo-induced h^+ jointly attack the organic pollutant.

A wide range of piezocatalysts have been developed for PS-AOPs, including $BaTiO_3$ [130], CNTs/$BaTiO_3$ [131], $Bi_2Fe_4O_9$ [132], $SrBi_2B_2O_7$ [133], MoS_2 [134–136], Fe@MoS_2 [137], $SnWO_4$/ZnO [138], cobalt-doped ZnAl-layered double hydroxides (ZnAl-LDH) [139], MoS_2-embedded PVDF membrane (PVDF-M10) [140], and so on. For example, Su et al. fabricated $Bi_2Fe_4O_9$ nanosheets (BFO NSs) and utilized them as piezocatalysts for PDS activation to eliminate BPA (Fig. 8b) [132]. It was discovered that the BFO NSs showed

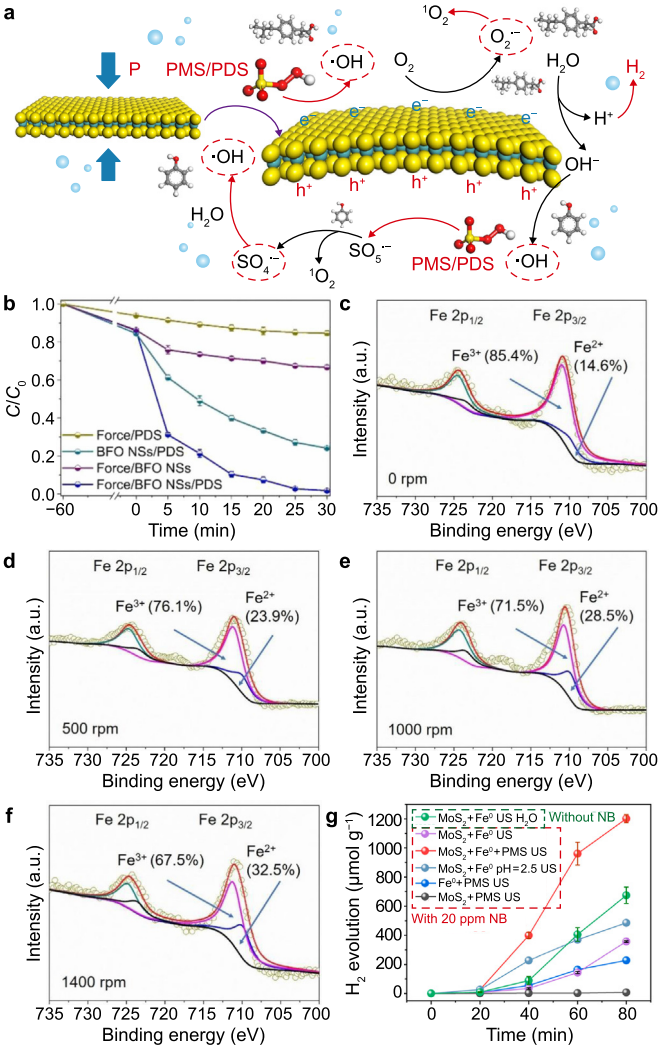

Fig. 8. a, Schematic illustration of the principle of piezocatalysis coupled with persulfate-based advanced oxidation processes. P: the polarization field, PMS: peroxymonosulfate, PDS: peroxydisulfate. **b,** Degradation of bisphenol A in different systems. BFO NSs: $Bi_2Fe_4O_9$ nanosheets. **c–f,** The X-ray photoelectron spectroscopy spectra of Fe 2p under 0 rpm (**c**), 500 rpm (**d**), 1000 rpm (**e**), and 1400 rpm (**f**) stirring. Adapted with permission from Ref. [132], Copyright 2022, Elsevier. **g,** The piezocatalytic H_2 yield curves of MoS_2/Fe^0, MoS_2/Fe^0/peroxymonosulfate, and MoS_2/Fe^0 (pH = 2.5) in nitrobenzene solution. US: ultrasound, NB: nitrobenzene. Adapted with permission from Ref. [141], Copyright 2023, PNAS.

chemical activity toward PDS activation, and the BFO NSs/PDS system achieved a BPA removal efficiency of 75.8%. However, the BPA removal efficiency was increased to 98.3% under magnetic stirring at a high speed, and the degradation rate constant achieved by the force/BFO NSs/PDS system was 3.1 times higher than that attained by the BFO NSs/PDS system. These results demonstrate that PDS can be piezocatalytically activated over BFO NSs, and that the synergy between piezocatalysis and PS-AOPs significantly improves the oxidation of organic pollutants.

Moreover, an XPS analysis revealed that the content of Fe^{2+} in used BFO NSs after the piezocatalytic activation process (force/BFO NSs/PDS system) was much higher than that in used BFO NSs after the catalytic activation process (BFO NSs/PDS system). Especially in the case of the force/BFO NSs/PDS system, the Fe^{2+} content of the piezocatalyst increased with stirring speed (Fig. 8c–f). These phenomena show that piezo-induced e^- can boost Fe^{3+}/Fe^{2+} circulation in BFO NSs, improving PDS activation performance. Several

types of ROS were produced in the force/BFO NSs/PDS system including $SO_4^{\bullet-}$, •OH, and $^1O_2$ while $SO_4^{\bullet-}$ and •OH made a major contribution to BPA oxidation, possibly due to the higher selectivity of $SO_4^{\bullet-}$ and •OH toward BPA than $^1O_2$.

As mentioned earlier in section 4.1, water can be decomposed into H_2, an important gas fuel via piezocatalysis. However, during the piezocatalytic degradation of organic pollutant processes, the H_2 yield is relatively low because the pollutant would inevitably consume electrons and suppress the H_2 evolution performance [141]. Recently, Xing's group discovered that coupling piezocatalysis with PS-AOPs can overcome this problem and realize simultaneous wastewater treatment and fuel production. This is significant to realizing carbon neutrality in environmental remediation [141]. They fabricated a coupled ternary MoS_2/Fe^0/PMS system to remove organic pollutants and measured the accompanied H_2 production [141]. It was found that the ternary system can completely remove nitrobenzene (NB) and achieve a H_2 production rate of 901.0 μmol g^{-1} h^{-1} under US vibration, which is much higher than that achieved by MoS_2/Fe^0/US system in pure water and is 2.03 times the summed H_2 yield in the NB solution of MoS_2/Fe^0, Fe^0/PMS and MoS_2/PMS systems under US (Fig. 8g).

This suggests a remarkable promotional effect of PMS on piezocatalytic H_2 evolution over MoS_2 in wastewater. The excellent H_2 evolution reaction performance manifested by the piezocatalytic MoS_2/Fe^0/PMS system is primarily attributed to the following two reasons: (i) Fe^0 serves as a good cocatalyst to improve the charge separation efficiency in MoS_2; (ii) the presence of PMS enhanced H^+ adsorption on the surface of MoS_2 and further boosted the subsequent evolution of the adsorbed H^+ ions into H_2, as consolidated by theoretical calculations. The same group also reported that a coupled piezocatalytic Co_3S_4/MoS_2/PMS system can realize simultaneous organic pollutant removal and selective CO production in actual wastewater treatment by exploiting the reactions between piezo-induced electrons and as-obtained carbonate from the oxidation of organics by PMS-AOPs, which provides a feasible approach to reduce the CO_2 emission in sewage treatment plant [142].

5. Conclusion and outlook

Piezocatalysis has been demonstrated to be a green, energy-saving water treatment technique. High-frequency vibrations (e.g., US, and ball milling) and low-frequency vibrations (e.g., air bubbling, and water vortex disturbance) can initiate the piezocatalytic degradation of aqueous organic pollutants. Furthermore, piezocatalysis can be integrated with other advanced oxidation techniques to achieve enhanced degradation performance owing to the peculiar functions of piezopotential and piezo-induced free-charge carriers. Hence, piezocatalysis is gaining widespread popularity in environmental remediation and is predicted to quickly climb to prominence.

Although substantial progress has been achieved in piezocatalysis research, this topic is still in its infancy, with many unresolved obstacles:

(i) Massive efforts have been made to improve piezocatalysts' efficiency via modifications. At the same time, fundamental analyses of the piezocatalysis process are limited, and the intrinsic mechanism of piezocatalysis is far from being elucidated. What is the exact source of charge carriers in piezocatalytic reactions? How does one piezoelectric material's catalytic activity differ from another? Why does one piezocatalyst show distinct activity in different reactions? Borrowing insights from well-developed research areas such piezoelectricity, piezotronics, and electrochemistry is very helpful in elucidating the piezocatalytic mechanism. More further in-depth experimental investigation, especially *in situ* tests combined with theoretical calculations, is necessary to unambiguously disclose the fundamentals of an observed piezocatalytic phenomenon. A full understanding of the piezocatalytic mechanism would boost the use of piezocatalysis as a green, sustainable environmental remediation technology.

(ii) More attempts should be made to enhance the performance of piezocatalysis driven by low-frequency mechanical energy for water remediation. Most current studies have employed high-frequency US waves more often than low-frequency mechanical energy to initiate piezocatalytic reactions due to the much lower catalytic efficiency in the latter case. Nevertheless, US waves normally need to be manufactured artificially with significant energy consumption, which is somewhat against the original motivation of using piezocatalysis to harvest natural energy. Hence, strategies for improving the utilization efficiency of low-frequency mechanical energy for piezocatalysis-based water treatment are urgently needed. One possible way is to fabricate monolithic piezocatalysts (e.g., films, foams, hydrogels) because monolithic piezocatalysts are more sensitive to low-frequency mechanical energy and are easier to recover than powdery materials. Additionally, the rational design of the architecture of piezocatalytic reactors instead of beaker experiments can better use hydromechanical energy.

(iii) Developing novel piezocatalysis-coupled water treatment technologies is significant. Due to the peculiar ability of piezopotential to regulate the band structure and interfacial charge transfer process, it has been assumed that piezocatalysis can also be combined with electrochemical techniques to achieve improved water treatment performance, while relevant studies are rarely documented. Also, coupling piezocatalysis with micro-nanobubble technology for water treatment is appealing because bubble cavitation is an effective mechanical stimulus for initiating piezocatalytic reactions. Particularly, the mass transfer and

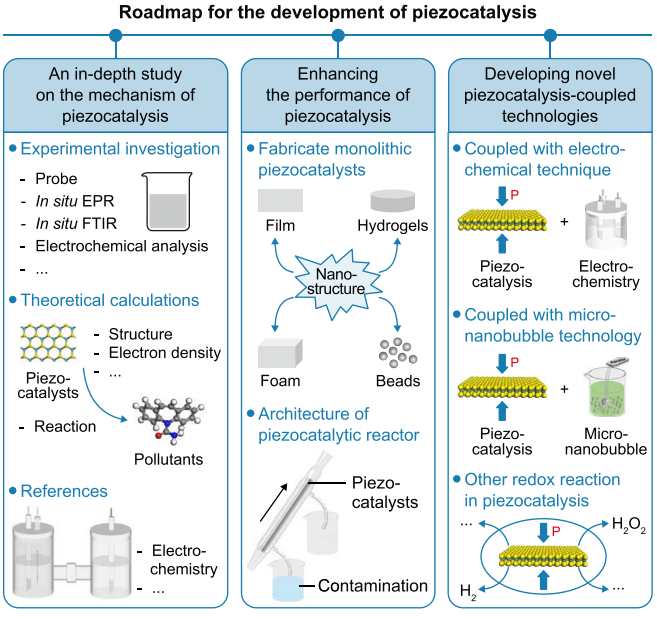

Fig. 9. The roadmap for piezocatalysis development. EPR: electron paramagnetic resonance, FTIR: fourier transform infrared spectroscopy, P: the polarization field.

thermodynamics of reactions in a coupled system are likely to be different from those in a single system since a three-phase (gas, solid, and liquid) interface is present in a coupled system. In this regard, piezocatalysis-micro-nanobubble technology is expected to manifest remarkable performance.

(iv) Finally, more attention should be given to the generation of value-added products (e.g., H_2O_2, H_2) from piezocatalysis or piezocatalysis-coupled water treatment technologies, which can contribute to the reduction of indirect carbon emissions in the wastewater treatment industry in the coming carbon-neutral era.

There is a long way to go before the practical applications of piezocatalysis in real-world water remediation, and ongoing input from the scientific community is necessary to develop and mature this research area (Fig. 9). We hope this current study offers clues regarding the direction that research on piezocatalysis-based water remediation should take to meet the goals of carbon peaking and carbon neutralization.

CRediT authorship contribution statement

Tian Jiang: Writing - Original Draft, Software, Methodology. **Yuehan Wang:** Software, Methodology. **Chang Cai:** Validation, Software. **Chunyang Nie:** Writing - Review & Editing, Supervision, Methodology, Funding Acquisition, Conceptualization. **Honggen Peng:** Writing - Review & Editing, Supervision. **Zhimin Ao:** Writing - Review & Editing, Supervision, Funding Acquisition, Conceptualization.

Declaration of competing interest

The authors declare that they have no known competing financial interests or personal relationships that could have appeared to influence the work reported in this paper.

Acknowledgement

This work was supported by the National Natural Science Foundation of China (grant No. 22166025 and 22176041), Jiangxi Natural Science Foundation (grant No. 20232BAB203037), and the National Key R&D Program of China (No. 2022YFC3901800).

References

[1] X. Yang, J. Duan, X. Zhang, H. Zhang, X. Liu, Y. Feng, M. Zheng, Heterojunction architecture of Nb_2O_5/g-C_3N_4 for enhancing photocatalytic activity to degrade organic pollutants and deactivate bacteria in water, Chin. Chem. Lett. 33 (8) (2022) 3792–3796, https://doi.org/10.1016/j.cclet.2021.11.031.

[2] S. Li, P.L. Show, H.H. Ngo, S.-H. Ho, Algae-mediated antibiotic wastewater treatment: a critical review, Environ. Sci. Ecotechnol. 9 (2022) 100145, https://doi.org/10.1016/j.ese.2022.100145.

[3] Y. Shi, D. Yang, C. Hu, L. Lyu, Water self-purification via electron donation effect of emerging contaminants arousing oxygen activation over ordered carbon-enhanced CoFe quantum dots, Environ. Sci. Ecotechnol. 20 (2024) 100356, https://doi.org/10.1016/j.ese.2023.100356.

[4] R. Guo, Y. Chen, Y. Yang, J. Shang, X. Cheng, Efficient degradation of sulfacetamide by CoFe PBAs and PBA@PVDF composite membrane activating peroxymonosulfate, Chin. Chem. Lett. 34 (5) (2023) 107837, https://doi.org/10.1016/j.cclet.2022.107837.

[5] C. Qin, J. Tang, R. Qiao, S. Lin, Tetracycline sensitizes TiO_2 for visible light photocatalytic degradation via ligand-to-metal charge transfer, Chin. Chem. Lett. 33 (12) (2022) 5218–5222, https://doi.org/10.1016/j.cclet.2022.01.067.

[6] B. Yang, X. Cheng, Y. Zhang, W. Li, J. Wang, H. Guo, Insight into the role of binding interaction in the transformation of tetracycline and toxicity distribution, Environ. Sci. Ecotechnol. 8 (2021) 100127, https://doi.org/10.1016/j.ese.2021.100127.

[7] J. Wang, S. Wang, Reactive species in advanced oxidation processes: formation, identification and reaction mechanism, Chem. Eng. J. 401 (2020), https://doi.org/10.1016/j.cej.2020.126158.

[8] X. Duan, H. Sun, S. Wang, Metal-free carbocatalysis in advanced oxidation reactions, Accounts Chem. Res. 51 (3) (2018) 678–687, https://doi.org/10.1021/acs.accounts.7b00535.

[9] Y. Li, M. Fan, C. Wang, Y. Li, X. Yu, J. Ding, L. Yan, L. Qiu, Y. Zhang, L. Wang, 3D layer-by-layer amorphous MoS_x assembled from $[Mo_3S_{13}]^{2-}$ clusters for efficient removal of tetracycline: synergy of adsorption and photo-assisted PMS activation, Chin. Chem. Lett. 35 (9) (2024) 109764, https://doi.org/10.1016/j.cclet.2024.109764.

[10] C. Wang, Y. Li, M. Fan, X. Yu, J. Ding, L. Yan, G. Qin, J. Yang, Y. Zhang, Controllable growth of silver nanoparticles on titanium dioxide/nitrogen-doped carbon nanofiber/molybdenum disulfide: toward enhanced photocatalytic-activating peroxymonosulfate performance and “memory catalysis”, Chem. Eng. J. 479 (2024) 147752 https://doi.org/10.1016/j.cej.2023.147752.

[11] Y. Wang, H. Zhao, S. Chai, Y. Wang, G. Zhao, D. Li, Electrosorption enhanced electro-Fenton process for efficient mineralization of imidacloprid based on mixed-valence iron oxide composite cathode at neutral pH, Chem. Eng. J. 223 (2013) 524–535, https://doi.org/10.1016/j.cej.2013.03.016.

[12] I. Sirés, E. Brillas, M.A. Oturan, M.A. Rodrigo, M. Panizza, Electrochemical advanced oxidation processes: today and tomorrow. A review, Environ. Sci. Pollut. Control Ser. 21 (14) (2014) 8336–8367, https://doi.org/10.1007/s11356-014-2783-1.

[13] C. Xiao, J. Yuan, L. Li, N. Zhong, D. Zhong, Q. Xie, H. Chang, Y. Xu, X. He, M. Li, Photocatalytic synergistic biofilms enhance tetracycline degradation and conversion, Environ. Sci. Ecotechnol. 14 (2023) 100234, https://doi.org/10.1016/j.ese.2022.100234.

[14] W. Liu, P. Wang, J. Chen, X. Gao, H. Che, X. Su, B. Liu, Y. Ao, In situ single iron atom doping on Bi_2WO_6 monolayers triggers efficient photo-fenton reaction, Environ. Sci. Ecotechnol. 20 (2024) 100414, https://doi.org/10.1016/j.ese.2024.100414.

[15] S. Li, C. You, K. Rong, C. Zhuang, X. Chen, B. Zhang, Chemically bonded $Mn_{0.5}Cd_{0.5}S$/BiOBr S-scheme photocatalyst with rich oxygen vacancies for improved photocatalytic decontamination performance, Adv. Powder Mater. 3 (3) (2024) 100183, https://doi.org/10.1016/j.apmate.2024.100183.

[16] K. Dong, C. Shen, R. Yan, Y. Liu, C. Zhuang, S. Li, Integration of plasmonic effect and S-scheme heterojunction into Ag/Ag_3PO_4/C_3N_5 photocatalyst for boosted photocatalytic levofloxacin degradation, Acta Phys. - Chim. Sin. 0 (0) (2023) 2310013, https://doi.org/10.3866/pku.whxb202310013.

[17] Y. Wang, D. Yu, Y. Liu, X. Liu, Y. Shi, Boosting piezo/photo-induced charge transfer of CNT/$Bi_4O_5I_2$ catalyst for efficient ultrasound-assisted degradation of rhodamine B, Materials 14 (16) (2021), https://doi.org/10.3390/ma14164449.

[18] W. Feng, J. Yuan, F. Gao, B. Weng, W. Hu, Y. Lei, X. Huang, L. Yang, J. Shen, D. Xu, X. Zhang, P. Liu, S. Zhang, Piezopotential-driven simulated electrocatalytic nanosystem of ultrasmall MoC quantum dots encapsulated in ultrathin N-doped graphene vesicles for superhigh H_2 production from pure water, Nano Energy 75 (2020), https://doi.org/10.1016/j.nanoen.2020.104990.

[19] K. Wang, C. Han, J. Li, J. Qiu, J. Sunarso, S. Liu, The mechanism of piezocatalysis: energy band theory or screening charge effect? Angew. Chem. Int. Ed. 61 (6) (2021) https://doi.org/10.1002/anie.202110429.

[20] W. Wu, C. Pan, Y. Zhang, X. Wen, Z.L. Wang, Piezotronics and piezo-phototronics – from single nanodevices to array of devices and then to integrated functional system, Nano Today 8 (6) (2013) 619–642, https://doi.org/10.1016/j.nantod.2013.11.002.

[21] G. Gautschi, Piezoelectric sensorics: force, strain, pressure, acceleration and acoustic emission sensors, materials and amplifiers, Sens. Rev. (2002) 363–364, https://doi.org/10.1108/sr.2002.22.4.363.2.

[22] K.-S. Hong, H. Xu, H. Konishi, X. Li, Direct water splitting through vibrating piezoelectric microfibers in water, J. Phys. Chem. Lett. 1 (6) (2010) 997–1002, https://doi.org/10.1021/jz100027t.

[23] Z. Ren, F. Chen, Q. Zhao, G. Zhao, H. Li, W. Sun, H. Huang, T. Ma, Efficient CO_2 reduction to reveal the piezocatalytic mechanism: from displacement current to active sites, Appl. Catal. B Environ. 320 (2023) 122007, https://doi.org/10.1016/j.apcatb.2022.122007.

[24] Y. Zhang, Q. An, S. Zhang, Z. Ma, X. Hu, M. Feng, Y. Zhang, Y. Zhao, A healing promoting wound dressing with tailor-made antibacterial potency employing piezocatalytic processes in multi-functional nanocomposites, Nanoscale 14 (7) (2022) 2649–2659.

[25] H. Lin, Z. Wu, Y. Jia, W. Li, R.-K. Zheng, H. Luo, Piezoelectrically induced mechano-catalytic effect for degradation of dye wastewater through vibrating $Pb(Zr_{0.52}Ti_{0.48})O_3$ fibers, Appl. Phys. Lett. 104 (16) (2014), https://doi.org/10.1063/1.4873522.

[26] J. Wu, N. Qin, D. Bao, Effective enhancement of piezocatalytic activity of $BaTiO_3$ nanowires under ultrasonic vibration, Nano Energy 45 (2018) 44–51, https://doi.org/10.1016/j.nanoen.2017.12.034.

[27] Q. Liu, F. Zhan, H. Luo, X. Luo, Q. Yi, Q. Sun, Z. Xiao, Y. Zhang, D. Zhang, C.R. Bowen, Na-Sm bimetallic regulation and band structure engineering in $CaBi_2Nb_2O_9$ to enhance piezo-photo-catalytic performance, Adv. Funct. Mater. (2023), https://doi.org/10.1002/adfm.202303736.

[28] H. Gao, Y. Zhang, H. Xia, X. Mao, X. Zhu, S. Miao, M. Shi, S. Zha, The Piezo-Fenton synergistic effect of ferroelectric single-crystal $BaTiO_3$ nanoparticles for high-efficiency catalytic pollutant degradation in aqueous solution, Dalton Trans. 51 (31) (2022) 11876–11883, https://doi.org/10.1039/d2dt01248k.

[29] N. Li, M. Shi, G. Sun, M. Wu, Q. Li, W. Shen, J. Ma, Z-scheme $CdIn_2S_4/Bi_2WO_6$ heterojunction for high piezo-photo synergetic performance, Inorg. Chem. 62 (21) (2023) 8261–8270, https://doi.org/10.1021/acs.inorgchem.3c00690.
[30] J. Ding, L. Bu, B. Cui, G. Zhao, Q. Gao, L. Wei, Q. Zhao, D.D. Dionysiou, Assessment of solar-assisted electrooxidation of bisphenol AF and bisphenol A on boron-doped diamond electrodes, Environ. Sci. Ecotechnol. 3 (2020) 100036, https://doi.org/10.1016/j.ese.2020.100036.
[31] Y. Cheng, Y. Zhang, Z. Wang, R. Guo, J. You, H. Zhang, Review of Bi-based catalysts in piezocatalytic, photocatalytic and piezo-photocatalytic degradation of organic pollutants, Nanoscale 15 (46) (2023) 18571–18580, https://doi.org/10.1039/d3nr05016e.
[32] A.K. Kole, S. Karmakar, A. Pramanik, P. Kumbhakar, Transition metal dichalcogenides nanomaterials based piezocatalytic activity: recent progresses and outlook, Nanotechnology 34 (28) (2023) 282001, https://doi.org/10.1088/1361-6528/accb5f.
[33] D. Masekela, N.C. Hintsho-Mbita, S. Sam, T.L. Yusuf, N. Mabuba, Application of $BaTiO_3$-based catalysts for piezocatalytic, photocatalytic and piezo-photocatalytic degradation of organic pollutants and bacterial disinfection in wastewater: a comprehensive review, Arab. J. Chem. 16 (2) (2023) 104473, https://doi.org/10.1016/j.arabjc.2022.104473.
[34] D. Mondal, S. Roy, S. Bardhan, J. Roy, I. Kanungo, R. Basub, S. Das, Recent advances in piezocatalytic polymer nanocomposites for wastewater remediation, Dalton Trans. 51 (2022), https://doi.org/10.1039/d1dt02653d.
[35] A. Ali, L. Chen, M.S. Nasir, C. Wu, B. Guo, Y. Yang, Piezocatalytic removal of water bacteria and organic compounds: a review, Environ. Chem. Lett. 21 (2) (2022) 1075–1092, https://doi.org/10.1007/s10311-022-01537-3.
[36] X. Chen, J. Wang, Z. Wang, H. Xu, C. Liu, B. Huo, F. Meng, Y. Wang, C. Sun, Low-frequency mechanical energy in the environment for energy production and piezocatalytic degradation of organic pollutants in water: a review, J. Water Proc. Eng. 56 (2023) 104312, https://doi.org/10.1016/j.jwpe.2023.104312.
[37] C. Wang, C. Hu, F. Chen, T. Ma, Y. Zhang, H. Huang, Design strategies and effect comparisons toward efficient piezocatalytic system, Nano Energy 107 (2023) 108093, https://doi.org/10.1016/j.nanoen.2022.108093.
[38] Z. Yang, X. Shu, D. Guo, J. Wang, H. Bian, Y. Jia, Progress in the research on organic piezoelectric catalysts for dye decomposition, Int. J. Miner. Metall. Mater. 31 (2) (2024) 245–260, https://doi.org/10.1007/s12613-023-2773-8.
[39] Q. Zhang, Y. Jia, W. Wu, C. Pei, G. Zhu, Z. Wu, L. Zhang, W. Fan, Z. Wu, Review on strategies toward efficient piezocatalysis of $BaTiO_3$ nanomaterials for wastewater treatment through harvesting vibration energy, Nano Energy 113 (2023) 108507, https://doi.org/10.1016/j.nanoen.2023.108507.
[40] L. Zhou, L. Meng, H. Jia, Y. Lu, T. Liang, Y. Yuan, C. Liu, Z. Dong, L. Hu, P. Guan, Y. Zhou, M. Li, T. Wan, Z. Han, D. Chu, Recent advances in piezocatalysts for dye degradation, Adv. Sustain. Syst. (2024), https://doi.org/10.1002/adsu.202300652.
[41] J. Liu, W. Qi, M. Xu, T. Thomas, S. Liu, M. Yang, Piezocatalytic techniques in environmental remediation, Angew. Chem. Int. Ed. 62 (5) (2022), https://doi.org/10.1002/anie.202213927.
[42] R. Djellabi, M.F. Ordonez, F. Conte, E. Falletta, C.L. Bianchi, I. Rossetti, A review of advances in multifunctional $XTiO_3$ perovskite-type oxides as piezo-photocatalysts for environmental remediation and energy production, J. Hazard Mater. 421 (2022) 126792, https://doi.org/10.1016/j.jhazmat.2021.126792.
[43] Z. Jiang, X. Tan, Y. Huang, Piezoelectric effect enhanced photocatalysis in environmental remediation: state-of-the-art techniques and future scenarios, Sci. Total. Environ. 806 (2022) 150924, https://doi.org/10.1016/j.scitotenv.2021.150924.
[44] J. He, C. Dong, X. Chen, H. Cai, X. Chen, X. Jiang, Y. Zhang, A. Peng, M.A.H. Badsha, Review of piezocatalysis and piezo-assisted photocatalysis in environmental engineering, Crystals 13 (9) (2023) 1382, https://doi.org/10.3390/cryst13091382.
[45] S. Tu, Y. Guo, Y. Zhang, C. Hu, T. Zhang, T. Ma, H. Huang, Piezocatalysis and piezo-photocatalysis: catalysts classification and modification strategy, reaction mechanism, and practical application, Adv. Funct. Mater. 30 (48) (2020), https://doi.org/10.1002/adfm.202005158.
[46] W.T. Yein, Q. Wang, D.-S. Kim, Piezoelectric persulfate activation process for oxidative degradation of aqueous pollutants, Kor. J. Chem. Eng. (2024), https://doi.org/10.1007/s11814-024-00155-9.
[47] Z. Jiang, X. Tan, Y. Huang, Piezoelectric effect enhanced photocatalysis in environmental remediation: state-of-the-art techniques and future scenarios, Sci. Total Environ. 806 (Pt 4) (2022) 150924, https://doi.org/10.1016/j.scitotenv.2021.150924.
[48] Z. Li, S. Lan, M. Zhu, Piezoelectricity activates persulfate for water treatment: a perspective, Environ. Sci. Ecotechnol. 18 (2024) 100329, https://doi.org/10.1016/j.ese.2023.100329.
[49] K. Wang, C. Han, Z. Shao, J. Qiu, S. Wang, S. Liu, Perovskite oxide catalysts for advanced oxidation reactions, Adv. Funct. Mater. 31 (30) (2021), https://doi.org/10.1002/adfm.202102089.
[50] J. Shi, W. Zeng, Z. Dai, L. Wang, Q. Wang, S. Lin, Y. Xiong, S. Yang, S. Shang, W. Chen, L. Zhao, X. Ding, X. Tao, Y. Chai, Piezocatalytic foam for highly efficient degradation of aqueous organics, Small Sci. 1 (2) (2020), https://doi.org/10.1002/smsc.202000011.
[51] J. Wang, J. Yu, Q. Fu, H. Yang, Q. Tong, Z. Hao, G. Ouyang, Unprecedented nonphotomediated hole (h^+) oxidation system constructed from defective carbon nanotubes and superoxides, ACS Cent. Sci. 7 (2) (2021) 355–364, https://doi.org/10.1021/acscentsci.0c01600.
[52] R. Lei, X. Fu, N. Chen, Y. Chen, W. Feng, P. Liu, Cocatalyst engineering to weaken the charge screening effect over Au–$Bi_4Ti_3O_{12}$ for piezocatalytic pure water splitting, Catal. Sci. Technol. 12 (24) (2022) 7361–7368, https://doi.org/10.1039/d2cy01422j.
[53] H. Shi, Y. Liu, Y. Bai, H. Lv, W. Zhou, Y. Liu, D.-G. Yu, Progress in defect engineering strategies to enhance piezoelectric catalysis for efficient water treatment and energy regeneration, Separ. Purif. Technol. 330 (2024) 125247, https://doi.org/10.1016/j.seppur.2023.125247.
[54] S. Li, Z. Zhao, D. Yu, J.-Z. Zhao, Y. Su, Y. Liu, Y. Lin, W. Liu, H. Xu, Z. Zhang, Few-layer transition metal dichalcogenides (MoS_2, WS_2, and WSe_2) for water splitting and degradation of organic pollutants: understanding the piezocatalytic effect, Nano Energy 66 (2019), https://doi.org/10.1016/j.nanoen.2019.104083.
[55] W. Tian, J. Qiu, N. Li, D. Chen, Q. Xu, H. Li, J. He, J. Lu, Efficient piezocatalytic removal of BPA and Cr(VI) with SnS_2/CNFs membrane by harvesting vibration energy, Nano Energy 86 (2021), https://doi.org/10.1016/j.nanoen.2021.106036.
[56] H. You, Y. Jia, Z. Wu, X. Xu, W. Qian, Y. Xia, M. Ismail, Strong piezoelectrochemical effect of multiferroic $BiFeO_3$ square micro-sheets for mechanocatalysis, Electrochem. Commun. 79 (2017) 55–58, https://doi.org/10.1016/j.elecom.2017.04.017.
[57] M.B. Starr, J. Shi, X. Wang, Piezopotential-driven redox reactions at the surface of piezoelectric materials, Angew Chem. Int. Ed. Engl. 51 (24) (2012) 5962–5966, https://doi.org/10.1002/anie.201201424.
[58] C. Xiang, K.M. Papadantonakis, N.S. Lewis, Principles and implementations of electrolysis systems for water splitting, Mater. Horiz. 3 (3) (2016) 169–173, https://doi.org/10.1039/c6mh00016a.
[59] M.B. Starr, X. Wang, Fundamental analysis of piezocatalysis process on the surfaces of strained piezoelectric materials, Sci. Rep. 3 (2013) 2160, https://doi.org/10.1038/srep02160.
[60] M.B. Starr, J. Shi, X. Wang, Piezopotential-driven redox reactions at the surface of piezoelectric materials, Angew. Chem. Int. Ed. 51 (24) (2012) 5962–5966, https://doi.org/10.1002/anie.201201424.
[61] J. Wu, W. Wang, Y. Tian, C. Song, H. Qiu, H. Xue, Piezotronic effect boosted photocatalytic performance of heterostructured $BaTiO_3/TiO_2$ nanofibers for degradation of organic pollutants, Nano Energy 77 (2020), https://doi.org/10.1016/j.nanoen.2020.105122.
[62] J. Wu, Q. Xu, E. Lin, B. Yuan, N. Qin, S.K. Thatikonda, D. Bao, Insights into the role of ferroelectric polarization in piezocatalysis of nanocrystalline $BaTiO_3$, ACS Appl. Mater. Interfaces 10 (21) (2018) 17842–17849, https://doi.org/10.1021/acsami.8b01991.
[63] K.-S. Hong, H. Xu, H. Konishi, X. Li, Piezoelectrochemical effect: a new mechanism for azo dye decolorization in aqueous solution through vibrating piezoelectric microfibers, J. Phys. Chem. C 116 (24) (2012) 13045–13051, https://doi.org/10.1021/jp211455z.
[64] Y. Zheng, W. Zhuang, M. Zhao, J. Zhang, Y. Song, S. Liu, H. Zheng, C. Zhao, Role of driven approach on the piezoelectric ozonation processes: comparing ultrasound with hydro-energy as driving forces, J. Hazard Mater. 418 (2021) 126392, https://doi.org/10.1016/j.jhazmat.2021.126392.
[65] J. Li, L. Yu, M. Liu, Y. Xie, Y. Yu, Aeration-driven piezoelectric activation of peroxymonosulfate achieves effective mitigation of antibiotic resistance dissemination, Environ. Pollut. 347 (2024) 123687, https://doi.org/10.1016/j.envpol.2024.123687.
[66] M. Zhang, W. Guo, Y. Chen, D. He, A.B. Isaev, M. Zhu, Dissolved oxygen in aeration-driven piezo-catalytic for antibiotics pollutants removal in water, Chin. Chem. Lett. 34 (9) (2023) 108229, https://doi.org/10.1016/j.cclet.2023.108229.
[67] B. Huo, J. Wang, Z. Wang, X. Zhang, J. Yang, Y. Wang, J. Qi, W. Ma, F. Meng, Bubble-driven piezo-activation of E-MoS_2/PVDF piezoelectric microcapsule for antibiotic degradation with ultralow energy consumption, J. Clean. Prod. 419 (2023) 138333, https://doi.org/10.1016/j.jclepro.2023.138333.
[68] W. Xu, B. Jing, Q. Li, J. Cao, J. Zhou, J. Li, D. Li, Z. Ao, Bubble induced piezoelectric activation of peroxymonosulfate on BiOCl for formaldehyde degradation during the absorption process: a density functional theory study, J. Mater. Chem. A (2024), https://doi.org/10.1039/d4ta00332b.
[69] R. Herrmann-Heber, S.F. Reinecke, U. Hampel, Dynamic aeration for improved oxygen mass transfer in the wastewater treatment process, Chem. Eng. J. 386 (2020) 122068, https://doi.org/10.1016/j.cej.2019.122068.
[70] W. Hou, Z. Chen, L. Liu, Strong synergy of piezoelectric photocatalysis in PFC catalyzed by $BaTiO_3/Bi_2WO_6$ anode and with peroxymonosulfate to remove rhodamine B, J. Sol. Gel Sci. Technol. 104 (1) (2022) 125–137, https://doi.org/10.1007/s10971-022-05898-7.
[71] Y. Feng, H. Li, L. Ling, S. Yan, D. Pan, H. Ge, H. Li, Z. Bian, Enhanced photocatalytic degradation performance by fluid-induced piezoelectric field, Environ. Sci. Technol. 52 (14) (2018) 7842–7848, https://doi.org/10.1021/acs.est.8b00946.
[72] Y. Feng, L. Ling, Y. Wang, Z. Xu, F. Cao, H. Li, Z. Bian, Engineering spherical lead zirconate titanate to explore the essence of piezo-catalysis, Nano Energy 40 (2017) 481–486, https://doi.org/10.1016/j.nanoen.2017.08.058.
[73] K. Kubota, Y. Pang, A. Miura, Redox reactions of small organic molecules using ball milling and piezoelectric Materials, Science 366 (2019) 1500–1504, https://doi.org/10.1126/science.aay8224.
[74] F. Meng, W. Ma, Y. Wang, Z. Zhu, Z. Chen, G. Lu, A tribo-positive Fe@MoS_2 piezocatalyst for the durable degradation of tetracycline: degradation

mechanism and toxicity assessment, Environ. Sci.: Nano 7 (6) (2020) 1704–1718, https://doi.org/10.1039/d0en00284d.
[75] S.L. James, C.J. Adams, C. Bolm, D. Braga, P. Collier, T. Friscic, F. Grepioni, K.D. Harris, G. Hyett, W. Jones, A. Krebs, J. Mack, L. Maini, A.G. Orpen, I.P. Parkin, W.C. Shearouse, J.W. Steed, D.C. Waddell, Mechanochemistry: opportunities for new and cleaner synthesis, Chem. Soc. Rev. 41 (1) (2012) 413–447, https://doi.org/10.1039/c1cs15171a.
[76] F. Meng, W. Ma, C. Duan, X. Liu, Z. Chen, M. Wang, J. Gao, Z. Zhang, High efficient degradation of levofloxacin by edge-selectively Fe@3D-WS_2: self-renewing behavior and Degradation mechanism study, Appl. Catal. B Environ. 252 (2019) 187–197, https://doi.org/10.1016/j.apcatb.2019.04.020.
[77] D. Liu, C. Jin, F. Shan, J. He, F. Wang, Synthesizing $BaTiO_3$ nanostructures to explore morphological influence, kinetics, and mechanism of piezocatalytic dye degradation, ACS Appl. Mater. Interfaces 12 (15) (2020) 17443–17451, https://doi.org/10.1021/acsami.9b23351.
[78] Y. Qin, M. Zhu, Y. Tang, X. Chen, F. Wang, X. Fan, Strong alternating piezoelectric field enhanced the piezocatalytic degradation of carbamazepine by a 3-chromophore material $Cd_4BiO(BO_3)_3$ coupled ultrasound in water, Chem. Eng. J. 469 (2023) 143911, https://doi.org/10.1016/j.cej.2023.143911.
[79] C. Yu, M. Tan, Y. Li, C. Liu, R. Yin, H. Meng, Y. Su, L. Qiao, Y. Bai, Ultrahigh piezocatalytic capability in eco-friendly $BaTiO_3$ nanosheets promoted by 2D morphology engineering, J. Colloid Interface Sci. 596 (2021) 288–296, https://doi.org/10.1016/j.jcis.2021.03.040.
[80] X. Ning, A. Hao, Y. Cao, J. Hu, J. Xie, D. Jia, Effective promoting piezocatalytic property of zinc oxide for degradation of organic pollutants and insight into piezocatalytic mechanism, J. Colloid Interface Sci. 577 (2020) 290–299, https://doi.org/10.1016/j.jcis.2020.05.082.
[81] X. Xu, Y. Jia, L. Xiao, Z. Wu, Strong vibration-catalysis of ZnO nanorods for dye wastewater decolorization via piezo-electro-chemical coupling, Chemosphere 193 (2018) 1143–1148, https://doi.org/10.1016/j.chemosphere.2017.11.116.
[82] F. Mushtaq, X. Chen, M. Hoop, H. Torlakcik, E. Pellicer, J. Sort, C. Gattinoni, B.J. Nelson, S. Pané, Piezoelectrically enhanced photocatalysis with $BiFeO_3$ nanostructures for efficient water remediation, iScience 4 (2018) 236–246, https://doi.org/10.1016/j.isci.2018.06.003.
[83] J. Wu, N. Qin, E. Lin, B. Yuan, Z. Kang, D. Bao, Synthesis of $Bi_4Ti_3O_{12}$ decussated nanoplates with enhanced piezocatalytic activity, Nanoscale 11 (44) (2019) 21128–21136, https://doi.org/10.1039/c9nr07544e.
[84] J.M. Wu, W.E. Chang, Y.T. Chang, C.K. Chang, Piezo-catalytic effect on the enhancement of the ultra-high degradation activity in the dark by single- and few-layers MoS_2 nanoflowers, Adv. Mater. 28 (19) (2016) 3718–3725, https://doi.org/10.1002/adma.201505785.
[85] M.-H. Wu, J.-T. Lee, Y.J. Chung, M. Srinivaas, J.-M. Wu, Ultrahigh efficient degradation activity of singleand few-layered $MoSe_2$ nanoflowers in dark by piezo-catalyst effect, Nano Energy 40 (2017) 369–375, https://doi.org/10.1016/j.nanoen.2017.08.042.
[86] S. Masimukku, Y.-C. Hu, Z.-H. Lin, S.-W. Chan, T.-M. Chou, J.M. Wu, High efficient degradation of dye molecules by PDMS embedded abundant single-layer tungsten disulfide and their antibacterial performance, Nano Energy 46 (2018) 338–346, https://doi.org/10.1016/j.nanoen.2018.02.008.
[87] S. Wang, Z. Wu, J. Chen, J. Ma, J. Ying, S. Cui, S. Yu, Y. Hu, J. Zhao, Y. Jia, Lead-free sodium niobate nanowires with strong piezo-catalysis for dye wastewater degradation, Ceram. Int. 45 (9) (2019) 11703–11708, https://doi.org/10.1016/j.ceramint.2019.03.045.
[88] C. Jin, D. Liu, M. Li, Y. Wang, Z. He, M. Xu, X. Li, H. Ying, Y. Wu, Q. Zhang, Preparation of multifunctional PLZT nanowires and their applications in piezocatalysis and transparent flexible films, J. Alloys Compd. 811 (2019), https://doi.org/10.1016/j.jallcom.2019.152063.
[89] J.M. Wu, Y.-G. Sun, W.-E. Chang, J.-T. Lee, Piezoelectricity induced water splitting and formation of hydroxyl radical from active edge sites of MoS_2 nanoflowers, Nano Energy 46 (2018) 372–382, https://doi.org/10.1016/j.nanoen.2018.02.010.
[90] M. Pan, C. Zhang, J. Wang, J.W. Chew, G. Gao, B. Pan, Multifunctional piezoelectric heterostructure of $BaTiO_3$@Graphene: decomplexation of Cu-EDTA and recovery of Cu, Environ. Sci. Technol. 53 (14) (2019) 8342–8351, https://doi.org/10.1021/acs.est.9b02355.
[91] J. Wang, X. Zhou, J. Hao, Z. Wang, B. Huo, J. Qi, Y. Wang, F. Meng, Sustainable self-powered degradation of antibiotics using Fe_3O_4@MoS_2/PVDF modified pipe with superior piezoelectric activity: mechanism insight, toxicity assessment and energy consumption, Appl. Catal. B Environ. 331 (2023) 122655, https://doi.org/10.1016/j.apcatb.2023.122655.
[92] A.H. Mamaghani, F. Haghighat, C.-S. Lee, Photocatalytic oxidation technology for indoor environment air purification: the state-of-the-art, Appl. Catal. B Environ. 203 (2017) 247–269, https://doi.org/10.1016/j.apcatb.2016.10.037.
[93] K. Maeda, Metal-complex/Semiconductor hybrid photocatalysts and photoelectrodes for CO_2 reduction driven by visible light, Adv. Mater. 31 (25) (2019) e1808205, https://doi.org/10.1002/adma.201808205.
[94] H. Zhang, J. He, C. Zhai, M. Zhu, 2D Bi_2WO_6/MoS_2 as a new photo-activated carrier for boosting electrocatalytic methanol oxidation with visible light illumination, Chin. Chem. Lett. 30 (12) (2019) 2338–2342, https://doi.org/10.1016/j.cclet.2019.07.021.
[95] B. Zhang, X. He, C. Yu, G. Liu, D. Ma, C. Cui, Q. Yan, Y. Zhang, G. Zhang, J. Ma, Y. Xin, Degradation of tetracycline hydrochloride by ultrafine TiO_2 nanoparticles modified g-C_3N_4 heterojunction photocatalyst: influencing factors, products and mechanism insight, Chin. Chem. Lett. 33 (3) (2022) 1337–1342, https://doi.org/10.1016/j.cclet.2021.08.008.
[96] J. Zhong, H. Jiang, Z. Wang, Z. Yu, L. Wang, J.F. Mueller, J. Guo, Efficient photocatalytic destruction of recalcitrant micropollutants using graphitic carbon nitride under simulated sunlight irradiation, Environ. Sci. Ecotechnol. 5 (2021) 100079, https://doi.org/10.1016/j.ese.2021.100079.
[97] Y. Zhu, W. Zhao, B. Jing, J. Zhou, B. Cai, D. Li, Z. Ao, Density functional theory calculations on 2H-MoS_2 monolayer for HCHO degradation: piezoelectric-photocatalytic synergy, Chin. Chem. Lett. 34 (5) (2023) 107816, https://doi.org/10.1016/j.cclet.2022.107816.
[98] D. Yu, Z. Liu, J. Zhang, S. Li, Z. Zhao, L. Zhu, W. Liu, Y. Lin, H. Liu, Z. Zhang, Enhanced catalytic performance by multi-field coupling in $KNbO_3$ nanostructures: piezo-photocatalytic and ferro-photoelectrochemical effects, Nano Energy 58 (2019) 695–705, https://doi.org/10.1016/j.nanoen.2019.01.095.
[99] T. Sakthivel, G. Venugopal, A. Durairaj, S. Vasanthkumar, X. Huang, Utilization of the internal electric field in semiconductor photocatalysis: a short review, J. Ind. Eng. Chem. 72 (2019) 18–30, https://doi.org/10.1016/j.jiec.2018.12.034.
[100] Q. Liu, W. Zhao, Z. Ao, T. An, Photo-piezoelectric synergistic degradation of typical volatile organic compounds on $BaTiO_3$, Chin. Chem. Lett. 33 (1) (2022) 410–414, https://doi.org/10.1016/j.cclet.2021.06.059.
[101] X. Chen, L. Liu, Y. Feng, L. Wang, Z. Bian, H. Li, Z.L. Wang, Fluid eddy induced piezo-promoted photodegradation of organic dye pollutants in wastewater on ZnO nanorod arrays/3D Ni foam, Mater. Today 20 (9) (2017) 501–506, https://doi.org/10.1016/j.mattod.2017.08.027.
[102] H. Li, Y. Sang, S. Chang, X. Huang, Y. Zhang, R. Yang, H. Jiang, H. Liu, Z.L. Wang, Enhanced ferroelectric-nanocrystal-based hybrid photocatalysis by ultrasonic-wave-generated piezophototronic effect, Nano Lett. 15 (4) (2015) 2372–2379, https://doi.org/10.1021/nl504630j.
[103] M. Ismail, Z. Wu, L. Zhang, J. Ma, Y. Jia, Y. Hu, Y. Wang, High-efficient synergy of piezocatalysis and photocatalysis in bismuth oxychloride nanomaterial for dye decomposition, Chemosphere 228 (2019) 212–218, https://doi.org/10.1016/j.chemosphere.2019.04.121.
[104] D. Hong, W. Zang, X. Guo, Y. Fu, H. He, J. Sun, L. Xing, B. Liu, X. Xue, High piezo-photocatalytic efficiency of CuS/ZnO nanowires using both solar and mechanical energy for degrading organic dye, ACS Appl. Mater. Interfaces 8 (33) (2016) 21302–21314, https://doi.org/10.1021/acsami.6b05252.
[105] Z. Yao, H. Sun, S. Xiao, Y. Hu, X. Liu, Y. Zhang, Synergetic piezo-photocatalytic effect in a Bi_2MoO_6/BiOBr composite for decomposing organic pollutants, Appl. Surf. Sci. 560 (2021), https://doi.org/10.1016/j.apsusc.2021.150037.
[106] H. Lei, H. Zhang, Y. Zou, X. Dong, Y. Jia, F. Wang, Synergetic photocatalysis/piezocatalysis of bismuth oxybromide for degradation of organic pollutants, J. Alloys Compd. 809 (2019), https://doi.org/10.1016/j.jallcom.2019.151840.
[107] H. Lei, M. Wu, Y. Liu, F. Mo, J. Chen, S. Ji, Y. Zou, X. Dong, Built-in piezoelectric field improved photocatalytic performance of nanoflower-like Bi_2WO_6 using low-power white LEDs, Chin. Chem. Lett. 32 (7) (2021) 2317–2321, https://doi.org/10.1016/j.cclet.2020.12.019.
[108] Z. Zhao, L. Wei, S. Li, L. Zhu, Y. Su, Y. Liu, Y. Bu, Y. Lin, W. Liu, Z. Zhang, Exclusive enhancement of catalytic activity in $Bi_{0.5}Na_{0.5}TiO_3$ nanostructures: new insights into the design of efficient piezocatalysts and piezo-photocatalysts, J. Mater. Chem. A 8 (32) (2020) 16238–16245, https://doi.org/10.1039/c9ta14007g.
[109] D. Ding, Z. Li, S. Yu, B. Yang, Y. Yin, L. Zan, N.V. Myung, Piezo-photocatalytic flexible PAN/TiO_2 composite nanofibers for environmental remediation, Sci. Total Environ. 824 (2022) 153790, https://doi.org/10.1016/j.scitotenv.2022.153790.
[110] H. Lv, Y. Liu, P. Zhao, Y. Bai, W. Cui, S. Shen, Y. Liu, Z. Wang, D.-G. Yu, Insight into the superior piezophotocatalytic performance of $BaTiO_3$//ZnO Janus nanofibrous heterostructures in the treatment of multi-pollutants from water, Appl. Catal. B Environ. 330 (2023) 122623, https://doi.org/10.1016/j.apcatb.2023.122623.
[111] Z. Wang, M. Liu, F. Xiao, G. Postole, H. Zhao, G. Zhao, Recent advances and trends of heterogeneous electro-Fenton process for wastewater treatment-review, Chin. Chem. Lett. 33 (2) (2022) 653–662, https://doi.org/10.1016/j.cclet.2021.07.044.
[112] D. Shao, L. Zhang, S. Sun, W. Wang, Oxygen reduction reaction for generating H_2O_2 through a piezo-catalytic process over bismuth oxychloride, ChemSusChem 11 (3) (2018) 527–531, https://doi.org/10.1002/cssc.201702405.
[113] K. Wang, D. Shao, L. Zhang, Y. Zhou, H. Wang, W. Wang, Efficient piezocatalytic hydrogen peroxide production from water and oxygen over graphitic carbon nitride, J. Mater. Chem. A 7 (35) (2019) 20383–20389, https://doi.org/10.1039/c9ta06251c.
[114] Y. Wei, Y. Zhang, J. Miao, W. Geng, M. Long, In-situ utilization of piezo-generated hydrogen peroxide for efficient p-chlorophenol degradation by Fe loading bismuth vanadate, Appl. Surf. Sci. 543 (2021), https://doi.org/10.1016/j.apsusc.2020.148791.
[115] W. Lv, L. Kong, S. Lan, J. Feng, Y. Xiong, S. Tian, Enhancement effect in the piezoelectric degradation of organic pollutants by piezo-Fenton process, J. Chem. Technol. Biotechnol. 92 (1) (2017) 152–156, https://doi.org/10.1002/jctb.4981.
[116] S. Wang, J. Long, T. Jiang, L. Shao, D. Li, X. Xie, F. Xu, Magnetic Fe_3O_4/CeO_2/g-C_3N_4 composites with a visible-light response as a high efficiency Fenton photocatalyst to synergistically degrade tetracycline, Separ. Purif. Technol. 278 (2021) 119609, https://doi.org/10.1016/j.seppur.2021.119609.
[117] R. Li, Y. Guo, G. Ma, D.T. Sun, J. Lin, T. Xue, R. Qiu, S. Yan, S. Yang, Y. Wang,

Y. Hong, Y. Su, H. Wang, L. Peng, J. Li, Efficient degradation of organic contaminants via a novel iron-based poly(ionic liquid)/polydopamine composite as the heterogeneous Fenton catalyst, Environ. Sci.: Nano 10 (5) (2023) 1232–1243, https://doi.org/10.1039/d3en00001j.

[118] M. Chai, W. Tong, Z. Wang, Z. Chen, Y. An, Y. Zhang, Piezoelectric-Fenton degradation and mechanism study of Fe_2O_3/PVDF-HFP porous film drove by flowing water, J. Hazard Mater. 430 (2022) 128446, https://doi.org/10.1016/j.jhazmat.2022.128446.

[119] D. Sun, N. Iqbal, W. Liao, Y. Lu, X. He, K. Wang, B. Ma, Y. Zhu, K. Sun, Z. Sun, T. Li, Efficient degradation of MB dye by 1D $FeWO_4$ nanomaterials through the synergistic effect of piezo-Fenton catalysis, Ceram. Int. 48 (17) (2022) 25465–25473, https://doi.org/10.1016/j.ceramint.2022.05.225.

[120] Y. Zhu, J. Zhu, H. ShenTu, Y. Wei, J. Wei, L. Lei, Y. Li, T. Yu, Z. Li, Y. Hou, Deformation of charge density activated by conductive carbon with the piezoelectric effect of tourmaline for highly promoting Fe^{3+}/Fe^{2+} cycle in Fenton-like process, Appl. Catal. B Environ. 334 (2023) 122824, https://doi.org/10.1016/j.apcatb.2023.122824.

[121] L. Ge, J. Xiao, W. Liu, G. Ren, C. Zhou, J. Liu, J.J. Zou, Z. Yang, A piezo-fenton system with rapid iron cycling and hydrogen peroxide self-supply driven by ultrasound, Chem. Eur J. 28 (71) (2022), https://doi.org/10.1002/chem.202202494.

[122] S. Hu, Y. Li, C. Zang, X. Ma, B. Zhao, F. Chen, Piezoelectric field-promoted heterogeneous sono-Fenton performance of MoS_2/α-Fe_2O_3 heterojunction structure, Appl. Surf. Sci. 534 (2020), https://doi.org/10.1016/j.apsusc.2020.147499.

[123] Z.-a. Jia, Q.-r. Zeng, X. Zhang, W. Feng, Enhanced ultrasound-assisted pore-adjustable spherical imma-Fe_3O_4 catalytic-activated piezoelectric Fenton reaction for PDE-5i degradation, J. Environ. Chem. Eng. 11 (2) (2023) 109419, https://doi.org/10.1016/j.jece.2023.109419.

[124] Z. Duan, W. Zhang, M. Lu, Z. Shao, W. Huang, J. Li, Y. Li, J. Mo, Y. Li, C. Chen, Magnetic Fe_3O_4/activated carbon for combined adsorption and Fenton oxidation of 4-chlorophenol, Carbon 167 (2020) 351–363, https://doi.org/10.1016/j.carbon.2020.05.106.

[125] Y. Liu, N. Du, X. Liu, D. Yao, D. Wu, Z. Li, S. Mao, ZnS-embedded porous carbon for peroxydisulfate activation: enhanced electron transfer for bisphenol A degradation, Environ. Sci. Ecotechnol. 19 (2024) 100338, https://doi.org/10.1016/j.ese.2023.100338.

[126] J. Li, Y. Li, Z. Xiong, G. Yao, B. Lai, The electrochemical advanced oxidation processes coupling of oxidants for organic pollutants degradation: a mini-review, Chin. Chem. Lett. 30 (12) (2019) 2139–2146, https://doi.org/10.1016/j.cclet.2019.04.057.

[127] K. Tian, L. Hu, L. Li, Q. Zheng, Y. Xin, G. Zhang, Recent advances in persulfate-based advanced oxidation processes for organic wastewater treatment, Chin. Chem. Lett. 33 (10) (2022) 4461–4477, https://doi.org/10.1016/j.cclet.2021.12.042.

[128] F. Wang, W. Wang, S. Yuan, W. Wang, Z.-H. Hu, Comparison of UV/H_2O_2 and UV/PS processes for the degradation of thiamphenicol in aqueous solution, J. Photochem. Photobiol. Chem. 348 (2017) 79–88, https://doi.org/10.1016/j.jphotochem.2017.08.023.

[129] C. Nie, J. Wang, B. Cai, B. Lai, S. Wang, Z. Ao, Multifunctional roles of MoS_2 in persulfate-based advanced oxidation processes for eliminating aqueous organic pollutants: a review, Appl. Catal. B Environ. 340 (2024) 123173, https://doi.org/10.1016/j.apcatb.2023.123173.

[130] S. Lan, Y. Chen, L. Zeng, H. Ji, W. Liu, M. Zhu, Piezo-activation of peroxymonosulfate for benzothiazole removal in water, J. Hazard Mater. 393 (2020) 122448, https://doi.org/10.1016/j.jhazmat.2020.122448.

[131] Y. Zheng, W. Zhuang, X. Zhang, J. Xiang, X. Wang, Z. Song, Z. Cao, C. Zhao, Grape-like CNTs/$BaTiO_3$ nanocatalyst boosted hydraulic-driven piezo-activation of peroxymonosulfate for carbamazepine removal, Chem. Eng. J. 449 (2022) 137826, https://doi.org/10.1016/j.cej.2022.137826.

[132] C. Su, R. Li, C. Li, W. Wang, Piezo-promoted regeneration of Fe^{2+} boosts peroxydisulfate activation by $Bi_2Fe_4O_9$ nanosheets, Appl. Catal. B Environ. 310 (2022) 121330, https://doi.org/10.1016/j.apcatb.2022.121330.

[133] M. Zhu, X. Chen, Y. Tang, S. Hou, Y. Yu, X. Fan, Piezo-promoted persulfate activation by $SrBi_2B_2O_7$ for efficient sulfadiazine degradation from water, J. Hazard Mater. 437 (2022) 129359, https://doi.org/10.1016/j.jhazmat.2022.129359.

[134] C. Yu, J. He, S. Lan, W. Guo, M. Zhu, Enhanced utilization efficiency of peroxymonosulfate via water vortex-driven piezo-activation for removing organic contaminants from water, Environ. Sci. Ecotechnol. 10 (2022), https://doi.org/10.1016/j.ese.2022.100165.

[135] S. Liu, B. Jing, C. Nie, Z. Ao, X. Duan, B. Lai, Y. Shao, S. Wang, T. An, Piezoelectric activation of peroxymonosulfate by MoS_2 nanoflowers for the enhanced degradation of aqueous organic pollutants, Environ. Sci.: Nano 8 (3) (2021) 784–794, https://doi.org/10.1039/d0en01237h.

[136] S.Y. Lan, B.H. Jing, C. Yu, D.M. Yan, Z. Li, Z.M. Ao, M.S. Zhu, Protrudent iron single-atom accelerated interfacial piezoelectric polarization for self-powered water motion triggered fenton-like reaction, Small 18 (2) (2022) e2105279, https://doi.org/10.1002/smll.202105279.

[137] L. Xu, L. Liu, Piezo-photocatalytic fuel cell with atomic Fe@MoS_2 on CFC helical electrode has enhanced peroxymonosulfate activation, pollutant degradation and power generation, Appl. Catal. B Environ. 304 (2022) 120953, https://doi.org/10.1016/j.apcatb.2021.120953.

[138] X. Zhou, Y. Liu, Y. Miao, W. He, Y. Pan, A. Jing Li, J. Qin, H. Li, R. Yin, R. Qiu, Coupled radical and nonradical activation of peroxymonosulfate by the piezo-photocatalytic effect of α-$SnWO_4$/ZnO heterojunction to boost the degradation and detoxification of carbamazepine, Separ. Purif. Technol. 323 (2023) 124410, https://doi.org/10.1016/j.seppur.2023.124410.

[139] Y. Lu, C. Ding, J. Guo, W. Gan, P. Chen, R. Chen, Q. Ling, M. Zhang, P. Wang, Z. Sun, Cobalt-doped ZnAl-LDH nanosheet arrays as recyclable piezocatalysts for effective activation of peroxymonosulfate to degrade norfloxacin: non-radical pathways and theoretical calculation studies, Nano Energy 112 (2023) 108515, https://doi.org/10.1016/j.nanoen.2023.108515.

[140] E. Wu, Y. Yu, J. Hu, G. Ren, M. Zhu, Piezoelectric-channels in MoS_2-embedded polyvinylidene fluoride membrane to activate peroxymonosulfate in membrane filtration for wastewater reuse, J. Hazard Mater. 458 (2023) 131885, https://doi.org/10.1016/j.jhazmat.2023.131885.

[141] W. Liu, P. Fu, Y. Zhang, H. Xu, H. Wang, M. Xing, Efficient hydrogen production from wastewater remediation by piezoelectricity coupling advanced oxidation processes, Proc. Natl. Acad. Sci. U. S. A. 120 (7) (2023) e2218813120, https://doi.org/10.1073/pnas.2218813120.

[142] M. Ran, H. Xu, Y. Bao, Y. Zhang, J. Zhang, M. Xing, Selective production of CO from organic pollutants by coupling piezocatalysis and advanced oxidation processes, Angew. Chem. Int. Ed. 62 (22) (2023), https://doi.org/10.1002/anie.202303728.